Characterisation of Nuclear Detectors

Using γ -Ray Spectroscopy

Dharmendra Pradhan

B.Sc. (Hons.) Physics, 2nd year

Sri Sri University, Cuttack, Odisha

Project Guide:

Satya Samiran Nayak

ABSTRACT

This report focuses on the interpretation of energy levels of ^{116}In resulting from the thermal neutron excitation of ^{115}In during the internship at **Variable Energy Cyclotron Centre, Kolkata** from May 2025 to July 2025. It includes the essential information required to understand the spectral data obtained through nuclear detectors. Theoretical concepts were practically implemented to interpret gamma-ray spectra and identify nuclear energy states, using ^{152}Eu as the calibration source. Experimental data were obtained using 8 clover HPGe and 10 scintillation detectors. The result contribute to our understanding towards nuclear energy level configurations of ^{116}In.

Contents

Introduction

Gamma spectroscopy is a powerful technique used to identify and study the discrete energy levels of atomic nuclei. When an atomic nucleus absorbs energy, typically in the form of a neutron, it transitions to an excited state. This excited nucleus then de-excites by emitting gamma rays as it returns to a lower energy or ground state. These gamma rays carry crucial information about the internal structure and properties of the nucleus.

Historically, the analysis of gamma emissions [fig.1] allowed scientists to chart nuclear decay pathways and understand nuclear structure. By analyzing gamma ray energies and intensities, researchers can infer critical nuclear parameters such as energy levels, transition probabilities, spin, parity, and nuclear shapes. The data gathered from these observations have been instrumental in the development of nuclear models and decay schemes.
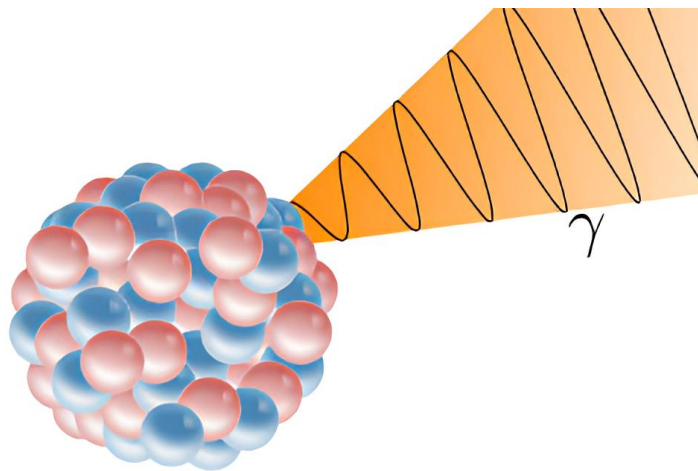
Figure 1: Gamma Emission

A specific focus of gamma spectroscopy is the investigation of nuclear rotation. When a non-rotating nucleus is excited, it may acquire angular momentum and exhibit rotational motion. The relationship between rotational energy and angular momentum typically follows a parabolic pattern. Examining this pattern allows researchers to determine the nature of nuclear motion and infer the shape of the nucleus. For instance, a symmetric rotational sequence often suggests a spherical nucleus, while deviations can indicate deformation.

The foundation of these observations lies in quantum mechanics. The wave function, usually denoted by ψ, describes the quantum state of particles such as nucleons. The square of its magnitude, $|\psi(x,t)|^2$, represents the probability density of finding the particle at a given location and time. Inside the nucleus, nucleons follow the Pauli exclusion principle, arranging themselves based on spin and energy in distinct shells. Each nucleon type (proton or neutron) has its own set of energy levels. The filling of these levels follows specific patterns—starting from the lowest energy configuration—much like electrons in atomic orbitals.

Nuclear stability is achieved by balancing the strong nuclear force and the electromagnetic repulsion between protons. As atomic number increases, stable configurations require more neutrons than protons. However, beyond a certain point, nuclei become unstable and undergo radioactive decay. Among various decay modes, gamma decay is often the most energy-efficient mechanism for an excited nucleus to release excess energy.

To detect gamma emissions, we rely on nuclear detectors, which act as our 'eyes' for observing otherwise invisible particles and radiation. Devices such as scintillation counters, Ge(Li) detectors, and HPGe detectors are commonly used to record the gamma spectra. These detectors measure energy deposition as channel numbers, which are proportional to the energy but not directly interpretable without calibration.

One of the nuclear reactions studied using gamma spectroscopy is $^{115}\text{In}(n, \gamma)^{116}\text{In}$. When a thermal or epithermal neutron is captured by ^{115}In, it forms an excited ^{116}In nucleus that emits prompt gamma rays during de-excitation. The energy distribution of these gamma rays provides insight into the nuclear structure of ^{116}In.

$$^{115}\text{In} + n_{\text{th}} \rightarrow\ ^{116}\text{In}^* \xrightarrow{\gamma}\ ^{116}\text{In}$$
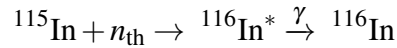
However, the raw data from detectors consist of channel numbers, not actual energies. To convert channel numbers to real energy values, energy calibration must be performed. In this work, calibration is carried out using a known standard source, ^{152}Eu, which emits gamma rays of precisely known energies. The peaks observed from this source are matched with their known energies, and a second-degree polynomial function is fitted to the data to determine calibration coefficients.

Once calibration parameters are obtained, unknown peaks in the $^{115}\text{In}(n, \gamma)$ spectrum can be accurately translated into energy values. This transformation is fundamental to further analysis, such as peak identification, efficiency correction, and comparison with theoretical or tabulated nuclear data.

Overall, this report presents the methodology and results of gamma spectral calibration using ^{152}Eu, laying the groundwork for future analysis of ^{116}In nuclear levels produced by neutron capture reactions.

Theoretical Interpretation

2.1   Wave Function

In quantum mechanics, a **wave function** is a mathematical function that describes the *quantum state* of a particle or system. Usually denoted by the Greek letter ψ, it contains all the information about a particle's behavior—such as its position, momentum, energy, and spin—in a given system. The square of the wave function's magnitude, $|\psi(x,t)|^2$, gives the *probability density* of finding the particle at a certain position and time.

In **nuclear physics**, the wave function is essential because the nucleus is a quantum system composed of protons and neutrons (nucleons), which obey the laws of quantum mechanics. Wave functions describe how nucleons are arranged and move within the nucleus, helping predict nuclear properties like spin, parity, and energy levels.

Note: that we can only separate the position and time aspect of a wave function when we are solving a time independent Schrödinger equation.

2.2   Normalisation

Normalization is a fundamental requirement in quantum mechanics, ensuring that the total probability of finding a particle within all space is equal to one. Since the square of the wave function's magnitude, $|\psi(x,t)|^2$, represents a probability density, the integral over all space must satisfy the condition:

$$\boxed{\int_{-\infty}^{\infty} |\psi(x,t)|^2\, dx = 1}$$

This condition guarantees that the particle described by the wave function exists somewhere in space. In nuclear physics, normalization is especially important when calculating measurable quantities like transition probabilities, matrix elements, and reaction cross sections, where properly normalized wave functions ensure accurate and physically meaningful results.

2.3   Derivation of Wave Equation

Time Dependent Wave Equation:

We know that,

$$E_{\text{Total}} = T_{\text{Kinetic}} + V_{\text{Potential}}$$

$$\Rightarrow E = \frac{p^2}{2m} + V(x) \tag{1.1}$$

We will use the following *de Broglie* relation to derive the Wave equation

$$E = \hbar\omega \quad \text{and} \quad p = \hbar k. \tag{1.2}$$

Applying the above relation in the Energy equation, we get:

$$\Rightarrow \hbar\omega = \frac{\hbar^2 k^2}{2m} + V(x). \tag{1.3}$$

To derive the wave equation, we can modify it by using a *wave function* $\Psi(x,t)$:

$$\Rightarrow \hbar\omega\,\Psi(x,t) = \frac{\hbar^2 k^2}{2m}\,\Psi(x,t) + V(x)\,\Psi(x,t). \tag{1.4}$$

Here, $\Psi(x,t)$ is a *wave function*. So, it can also be represented as

$$\Psi(x,t) = A e^{i(kx-\omega t)}. \tag{1.5}$$

If we differentiate the above equation with respect to position (x) and time (t) separately, then we get, the following relation which can be used in our energy equation:

$$\frac{\partial\Psi}{\partial t} = -i\omega\,\Psi(x,t) \quad \text{and} \quad \frac{\partial^2\Psi}{\partial x^2} = -k^2\,\Psi(x,t) \tag{1.6}$$

If we substitute both the value of kinetic energy term and total energy term (E):

$$\Rightarrow -\frac{\hbar}{i}\frac{\partial\Psi}{\partial t} = -\frac{\hbar^2}{2m}\frac{\partial^2\Psi}{\partial x^2} + V(x)\Psi(x,t) \tag{1.7}$$

$$\Rightarrow i\hbar\frac{\partial\Psi}{\partial t} = -\frac{\hbar^2}{2m}\frac{\partial^2\Psi}{\partial x^2} + V(x)\Psi(x,t) \tag{1.8}$$

Equation (1.8) is known as the **Time Dependent Schrödinger Equation**.

Time Independent Wave Equation:

To derive the Time Independent Schrödinger Equation, we use the method of *separation of variables*, assuming the total wave function can be written as:

$$\Psi(x,t) = \psi(x)\,f(t) \tag{2.1}$$

Substitute this into the Time Dependent Schrödinger Equation:

$$i\hbar\frac{\partial}{\partial t}\left[\psi(x)f(t)\right] = -\frac{\hbar^2}{2m}\frac{\partial^2}{\partial x^2}\left[\psi(x)f(t)\right] + V(x)\,\psi(x)f(t) \tag{2.2}$$

Apply the product rule:

$$i\hbar\psi(x)\frac{df(t)}{dt} = -\frac{\hbar^2}{2m}f(t)\frac{d^2\psi(x)}{dx^2} + V(x)\,\psi(x)f(t) \tag{2.3}$$

Divide both sides by $\psi(x)f(t)$:

$$i\hbar\frac{1}{f(t)}\frac{df(t)}{dt} = -\frac{\hbar^2}{2m}\frac{1}{\psi(x)}\frac{d^2\psi(x)}{dx^2} + V(x) \tag{2.4}$$

Since the left-hand side is a function of t only and the right-hand side is a function of x only, both must be equal to a constant, say E, which represents the total energy of the system.

So we get two separate equations:

$$i\hbar \frac{d\ f(t)}{dt} = E\ f(t) \tag{2.5}$$

$$-\frac{\hbar^2}{2m}\frac{d^2\psi(x)}{dx^2} + V(x)\,\psi(x) = E\,\psi(x) \tag{2.6}$$

Equation (2.6) is known as the **Time Independent Schrödinger Equation**.

2.4   Quantum Models

Particle in 1D Box

A **particle in a 1-dimensional box** is a fundamental quantum mechanical approximation describing the translational motion of a single particle confined inside an infinitely deep well from which it cannot escape. The **"Particle in a Box model"** is also known as the infinite potential well or the infinite square well [6].
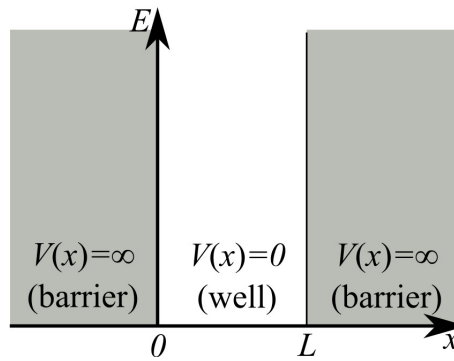
Figure 2: 1-D Infinite Potential Box

1. **Define the Potential Energy, V:**

   Potential energy is 0 inside the box ($V = 0$ for $0 < x < L$) and goes to infinity at the walls of the box ($V = \infty$ for $x < 0$ or $x > L$). We assume the walls have infinite potential energy to ensure that the particle has zero probability of being at the walls or outside the box.

2. **Solve the Schrödinger Equation:**

   Time-independent Schrödinger Equation for a particle of mass m, moving in one direction with energy E:

$$-\frac{\hbar^2}{2m}\frac{d^2\psi(x)}{dx^2} + V(x)\psi(x) = E\psi(x) \tag{3.1}$$

   Inside the box, where $V(x) = 0$:

$$-\frac{\hbar^2}{2m}\frac{d^2\psi(x)}{dx^2} = E\psi(x) \tag{3.2}$$

The general solution of this differential equation is:

$$\psi(x) = A\sin(kx) + B\cos(kx) \tag{3.3}$$

3. **Apply Boundary Conditions:** At $x = 0$:

$$\psi(0) = A\sin(0) + B\cos(0) = B \tag{3.4}$$

Since $\psi(0) = 0$, we must have $B = 0$. Therefore,

$$\psi(x) = A\sin(kx) \tag{3.5}$$

Differentiating twice:

$$\frac{d^2\psi(x)}{dx^2} = -k^2 A\sin(kx) = -k^2\psi(x) \tag{3.6}$$

Substitute into Equation (3.2):

$$-\frac{\hbar^2}{2m}(-k^2\psi(x)) = E\psi(x) \Rightarrow \frac{\hbar^2 k^2}{2m} = E \tag{3.7}$$

Solving for k:

$$k = \sqrt{\frac{2mE}{\hbar^2}} \tag{3.8}$$

Substitute into Equation (3.5):

$$\boxed{\psi(x) = A\sin\left(\sqrt{\frac{2mE}{\hbar^2}}x\right)} \tag{3.9}$$

4. **Define the Allowed Energies:**

   Apply boundary condition at $x = L$:

$$\psi(L) = A\sin\left(\sqrt{\frac{2mE}{\hbar^2}}L\right) = 0 \tag{3.10}$$

For this to be zero (and $A \neq 0$), the argument must be $n\pi$:

$$\sqrt{\frac{2mE}{\hbar^2}}L = n\pi \quad \text{where } n = 1, 2, 3, \ldots \tag{3.11}$$

Solving for energy E:

$$E_n = \frac{n^2\pi^2\hbar^2}{2mL^2} \tag{3.12}$$

The energy equation for particle in 1D box tells us:

- The energy of a particle is quantized.

- The lowest possible energy of a particle is not zero. This is called the Zero point energy and means the particle can never be at rest because it always has some kinetic energy.

- This is also consistent with the Heisenberg Uncertainty principle: If the particle had zero energy, we would know where it was in both space and time.

Harmonic Oscillator

A classical harmonic oscillator model describes a mass m attached to a spring with force constant k, governed by Hooke's law [2].

$$F = ma = m\frac{d^2x}{dt^2} \tag{4.1}$$

$$-kx = m\frac{d^2x}{dt^2} \tag{4.2}$$

$\therefore$ Solution of $x(t) = A\sin(\omega t) + B\cos(\omega t)$ where, average frequency of oscillation, $\omega = \sqrt{\dfrac{k}{m}}$

$$\Rightarrow \omega^2 m = k \tag{4.3}$$

$$V(x) = \frac{1}{2}kx^2 \tag{4.4}$$

We have to solve the time independent Schrödinger equation for the potential:

$$V(x) = \frac{1}{2}m\omega^2 x^2 \tag{4.5}$$

$$-\frac{\hbar^2}{2m}\frac{d^2\psi}{dx^2} + \frac{1}{2}m\omega^2 x^2 \psi = E\psi \tag{4.6}$$

$$\Rightarrow \frac{1}{2m}\left[\left(\hbar\frac{d}{dx}\right)^2 + (m\omega x)^2\right]\psi = E\psi \tag{4.7}$$

From Equation 4.7, we get two operators:

$$a_\pm = \frac{1}{\sqrt{2m}}\left(\hbar\frac{d}{dx} \pm im\omega x\right) \tag{4.8}$$

Now, compute the operator product $(a_- a_+)f(x)$:

$$(a_- a_+) f(x) = \frac{1}{\sqrt{2m}} \left(\hbar \frac{d}{dx} - im\omega x \right) \cdot \frac{1}{\sqrt{2m}} \left(\hbar \frac{d}{dx} + im\omega x \right) f(x) \tag{4.9}$$

$$= \frac{1}{2m} \left(\hbar \frac{d}{dx} - im\omega x \right) \left(\hbar \frac{df}{dx} + im\omega x f \right)$$

$$= \frac{1}{2m} \left[\hbar^2 \frac{d^2 f}{dx^2} + im\omega x \hbar \frac{df}{dx} - im\omega x \hbar \frac{df}{dx} - m^2 \omega^2 x^2 f + \hbar m \omega f \right]$$

$$= \frac{1}{2m} \left(\hbar^2 \frac{d^2 f}{dx^2} - m^2 \omega^2 x^2 f + \hbar m \omega f \right)$$

$$= \frac{1}{2m} \left(\hbar^2 \frac{d^2 f}{dx^2} + m^2 \omega^2 x^2 f \right) + \frac{1}{2} \hbar \omega f$$

Now, discarding the test function $f(x)$:

$$a_- a_+ = \frac{1}{2m} \left[\left(\hbar \frac{d}{dx} \right)^2 + (m\omega x)^2 \right] + \frac{1}{2} \hbar \omega \tag{4.10}$$

$$a_+ a_- = \frac{1}{2m} \left[\left(\hbar \frac{d}{dx} \right)^2 + (m\omega x)^2 \right] - \frac{1}{2} \hbar \omega \tag{4.11}$$

If we subtract Equation (4.11) from (4.10), we get:

$$a_- a_+ - a_+ a_- = \hbar \omega \tag{4.12}$$

We can also modify the time independent Schrödinger equation.

$$\left[a_+ a_- + \frac{1}{2} \hbar \omega \right] \psi = E \psi \qquad \text{or} \qquad \left[a_- a_+ - \frac{1}{2} \hbar \omega \right] \psi = E \psi \tag{4.13}$$

What will happen if we continuously apply a_- operator repeatedly? Eventually we are going to reach a state with energy less than 0, *which does not exist.* At some point machine must fail. We know that $a_- \psi$ is a solution to the Schrödinger equation. But that doesn't mean it will be normalizable as its value could be 0 or it's square would be ∞. There must be a lowest energy level, whose wavefunction will be ψ_0 such that $a_- \psi_0 = 0$.

To get the ground state energy value we put the value of $a_- \psi_0$ in equation (4.14),

$$\left[a_+ a_- + \frac{1}{2} \hbar \omega \right] \psi_0 = E \psi_0$$

$$\Rightarrow a_+ a_- \psi_0 + \frac{1}{2} \hbar \omega \psi_0 = E \psi_0$$

$$\Rightarrow \frac{1}{2} \hbar \omega \psi_0 = E \psi_0 \qquad \{ \text{ here, } a_- \psi_0 = 0 \}$$

$$\Rightarrow \frac{1}{2}\hbar\omega = E$$

$$\boxed{E_0 = \frac{1}{2}\hbar\omega} \tag{4.14}$$

Similarly using the raising operator, we get:

$$\boxed{E_n = \left(n + \frac{1}{2}\right)\hbar\omega} \tag{4.15}$$

Radioactive Decays

Radioactive decay refers to a group of reactions involving the nucleus of an atom changing in some form. Decay here implies gradual disappearance of a substance.

3.1 Why a decay occurs?

Nuclear stability is related to the balance of forces within the nucleus, specifically the strong nuclear force and the electromagnetic force. The ratio of neutrons to protons in a nucleus also plays a role in stability. For lighter elements, the ratio is close to 1:1, but as atomic number increases, the ratio shifts to favour more neutrons for stability.

As the number of protons in a nucleus increases, the repulsive electromagnetic force between them becomes stronger. For very large nuclei (high atomic numbers), this repulsion can overcome the strong nuclear force, making the nucleus unstable. To achieve nuclear stability (a more stable configuration), the nucleus will undergo radioactive decay.

Why doesn't the nucleus emit alpha or beta or simply emit a particle like neutron or proton? A nucleus becomes stable by the process that completes shortest. It would have emitted it's extra energies in the form of particle or alpha or beta particles if it had enough energy to do that. If it is undergoing gamma decay, then it means it is the best way it could release the extra energy [5].

3.2 Types of radioactive decay

A specific type of decay occurs because it is the best and fastest way to release the extra energy of the nucleus. So, there are mainly 3 types of process through which a nuclei becomes stable.

1. Alpha Decay

2. Beta Decay

3. Gamma Decay

Alpha Decay:

Through alpha decay a nucleus emits an alpha particle, which is essentially a helium nucleus *i.e.*, ^4_2He. This process results in reduction of atomic mass number and atomic number of original nuclei by 4 and 2 respectively. The general equation of α decay is given below:

$$^A_Z X \rightarrow ^{A-4}_{Z-2}Y + ^4_2\alpha$$
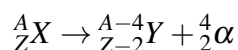
Beta Decay:

A beta decay is a process by which a beta particle (an electron or a positron) is emitted from an atomic nucleus after decay. Beta decay can occur in three processes i.e., β^- decay, β^+ decay or electron capture. This process either results in a proton to convert into a neutron and vice-versa.

i) β^- decay: When neutron inside an unstable atomic nucleus is converted into a proton, it's called β^- decay. One such example is the beta minus decay of ^{152}Eu to ^{152}Gd, where a neutron in the ***europium*** nucleus is converted into a proton, resulting in the formation of a ***gadolinium*** nucleus.
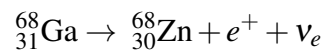
$$^{152}_{63}\text{Eu} \rightarrow \, ^{152}_{64}\text{Gd} + e^- + \bar{\nu}_e$$
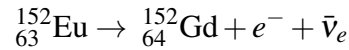
ii) β^+ decay: When proton inside an unstable atomic nucleus is converted into a neutron, it's called β^+ decay. One such example is the beta plus decay of ^{68}Ga to ^{68}Zn, where a proton in the ***gallium*** nucleus is converted into a neutron, resulting in the formation of a zinc nucleus.

$$^{68}_{31}\text{Ga} \rightarrow \, ^{68}_{30}\text{Zn} + e^+ + \nu_e$$

iii) EC or Electron capture decay: One such example is the electron capture decay of ^{152}Eu to ^{152}Sm, where a proton in the ***europium*** nucleus captures an inner orbital electron and is converted into a neutron, resulting in the formation of a ***samarium*** nucleus.

$$^{152}_{63}\text{Eu} + e^- \rightarrow \, ^{152}_{62}\text{Sm} + \nu_e$$
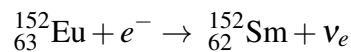
It can be very difficult to differentiate β^+ and electron capture decay as the daughter nuclei is same. But the fundamental difference is in β^+ decay as it emits an positron due to which it requires more energy (about 1 MeV) and as compared the nuclei absorbs an in shell electron to get a neutron in EC decay. Therefore, it is common to expect electron capture decay in heavier elements.

Gamma Decay:

Most of the times after a radioactive decay like α decay or β decay of the parent nuclei, it leaves the daughter nuclei in excited state. In this case the nuclei wants to seek a stable nuclear energy state i.e., ground state. To become stable the nuclei emits energy in form of a high energy photon or γ. In other words, γ is a photon which is essentially the energy that is emitted from an excited nuclide. **For example:** ^{152}Sm as a daughter nuclei emits gamma after it is formed after beta decay of ^{152}Eu.

$$^{152}_{62}\text{Sm}^* \rightarrow \, ^{152}_{62}\text{Sm} + \gamma \, (121 \text{ keV})$$
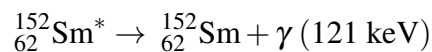
3.3   Factors Influencing Nuclear Decay

Several factors affect how a nucleus decays and which paths it follows during the process. Quantities like the hindrance factor, beta feeding, and branching ratio help describe the likelihood of different decay transitions, the population of nuclear energy levels, and how strongly certain decay paths are favored. These factors are useful for understanding decay patterns and the structure of the nucleus.

Alpha Hindrance Factor:

The alpha hindrance factor (HF) is a quantitative measure of how much slower the observed alpha decay of a nucleus is compared to the theoretically predicted rate. Specifically, it is defined as the ratio of the experimentally measured partial half-life of alpha decay to the calculated half-life based on quantum tunnelling models:

$$HF = \frac{Experimental\ partial\ half-life}{calculated\ half-life}$$

A hindrance factor greater than 1 indicates that the decay is "hindered," meaning it occurs more slowly than expected from simple models, usually due to additional nuclear structure effects such as differences in angular momentum, parity, or nuclear deformation between the parent and daughter nuclei.

Nuclear deformation refers to the deviation of a nucleus from a perfectly spherical shape. While the simplest model of the atomic nucleus assumes it is a sphere, in reality, many nuclei are not perfectly spherical—they can be elongated (prolate), flattened (oblate), or have even more complex shapes.

Causes of Nuclear Deformation: Nuclei with filled shells tend to be spherical, while those with partially filled shells may deform. The arrangement and interactions of protons and neutrons can favor non-spherical shapes to minimize energy. Nuclei in excited states are often more deformed than in their ground state.

Beta Feeding Intensity:

Beta feeding intensity (I_β) refers to the probability that a beta decay event populates a specific energy state in the daughter nucleus. It quantifies how frequently beta decay transitions from the parent nucleus ground state to a particular excited or ground state in the daughter nucleus occur. This intensity is expressed as a percentage or fraction of total beta decays.

The beta feeding intensity (or beta feeding probability) is the fraction of decays where beta (β^- or β^+) transitions directly populate a specific excited state of the daughter nucleus.

It tells us how much of the total beta decay goes into a particular level, before any gamma emission occurs.

Branching Ratio:

The branching ratio refers to the probability that a parent nucleus will decay through a specific decay mode or transition when multiple decay paths are available. It is expressed as a percentage or fraction of the total decay rate.

When a nucleus decays, it may populate different energy levels of the daughter nucleus depending on the decay mode (e.g., alpha, beta, or gamma decay). The branching ratio determines how often each possible transition occurs.

γ - Transition Mechanism

4.1 Nuclear Energy Levels

Nuclear energy levels refer to the discrete energy states that a nucleus can occupy, similar to how electrons in an atom have specific energy levels. These levels represent the energy of the nucleus as a whole, either in its ground state (lowest energy) or in excited states (higher energy levels). Nucleons (protons and neutrons) within the nucleus also have their own energy levels within the overall nuclear energy levels.

Naturally the nucleons arrange themselves in particular order depending on their spin, orbital angular momentum and their own respective energy. They also follow the Pauli's exclusion principle. And no two nucleon of the same spin can remain in same energy level. Also each type of nucleon has their own respective energy level i.e., neutron has it's own energy levels and so does proton. The nucleon having the least energy stay in the 1st energy level or shell. The 1st energy level has 2 nucleon and 2nd can store 6 nucleons and so on.

4.2 Why γ - transition occurs..

After a nucleus decays, the daughter nucleus is left in an excited state most of the time. For example, when ^{133}Ba decays through electron capture (EC), it produces ^{133}Cs. But the daughter nucleus remains in an excited state after the decay. In the above decay scheme figure (3) you can see its decay scheme. Therefore, it tries to de-excite by emitting energy in the form of γ rays. The energy levels that a nucleus attains are not continuous but discrete, as it is a quantum mechanical object. So, when it emits γ rays, it does so in a discrete manner while transitioning from one state to another until reaching the ground state energy.
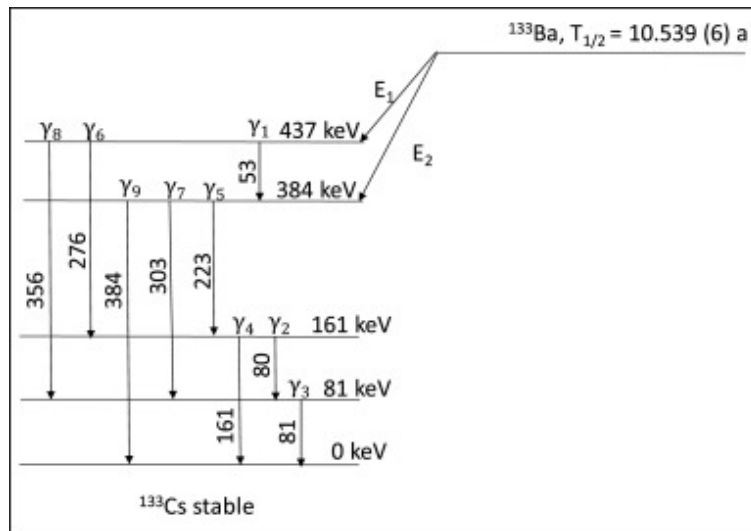

Figure 3: Decay Scheme of ^{133}Ba to ^{133}Cs
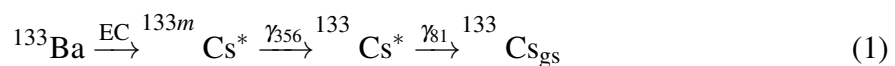
4.3 Gamma-Ray Coincidence

In nuclear decay, more than one gamma ray may be emitted from the same nucleus in a very short time. Therefore, analysis of gamma-ray coincidences is essential for interpreting complex
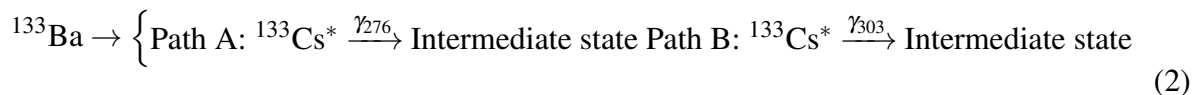
decay cascades, as it enables the identification of gamma rays emitted in correlated groups. This coincidence information is crucial for:

- Resolving which gamma transitions belong to the same decay path

- Verifying level schemes and spin assignments (*for example: figure (3)*)

- Isolated single transitions are particularly valuable for detector calibration

Coincident gamma transition: Coincident gamma rays are emitted in a correlated cascade from a nucleus, where multiple gamma transitions occur sequentially within a short time window. These are detected simultaneously in a coincidence measurement, allowing reconstruction of nuclear level schemes. A classic example is the decay of ^{133}Ba (fig.3), where the 356 keV γ-ray (from the ^{133m}Cs isomer) is often detected in coincidence with the 81 keV γ-ray through the decay sequence: ^{133}Ba $\rightarrow$ ^{133m}Cs (356 keV) $\rightarrow$ ^{133}Cs (81 keV) $\rightarrow$ ground state.

$$^{133}\text{Ba} \xrightarrow{EC} {}^{133m}\text{Cs}^* \xrightarrow{\gamma_{356}} {}^{133}\text{Cs}^* \xrightarrow{\gamma_{81}} {}^{133}\text{Cs}_{gs} \tag{1}$$

Parallel gamma transition: Parallel gamma transitions occur when a nucleus in an excited state decays via competing pathways to different lower-energy states, emitting only one gamma ray per decay event. In ^{133}Ba decay (fig.3), the 276 keV and 302 keV γ-rays represent parallel transitions from different initial states that populate the same intermediate level, but are never observed in coincidence with each other as they originate from separate decay branches.

$$^{133}\text{Ba} \rightarrow \left\{ \text{Path A: } {}^{133}\text{Cs}^* \xrightarrow{\gamma_{276}} \text{Intermediate state Path B: } {}^{133}\text{Cs}^* \xrightarrow{\gamma_{303}} \text{Intermediate state} \right. \tag{2}$$

Single gamma transition A single gamma transition occurs when an excited nucleus decays by emitting only one gamma ray without any coincident emissions. These transitions produce clean, isolated peaks in gamma spectra, making them ideal for detector calibration. The most prominent example is the 662 keV gamma ray from ^{137}Cs decay, which serves as a standard reference due to its well-defined energy, high emission probability (85%), and lack of interfering coincident transitions.

$$^{137}\text{Cs} \xrightarrow{\beta^-} {}^{137}\text{Ba}^* \xrightarrow{\gamma_{661.7\,keV}} {}^{137}\text{Ba}_{gs} \tag{3}$$

The 661.7 keV transition is particularly valuable for calibration because of its precise energy, long half-life (30.08 years), and the absence of cascade gamma rays that could complicate spectral analysis.

4.4 Multipolarity

Multipolarity describes the angular momentum (l) and parity (π) carried away by a gamma (γ) photon when a nucleus decays from an excited state to a lower energy state. It determines:

- The type of gamma transition (electric or magnetic)

- The change in nuclear spin (J) and parity (π)

- The probability (decay rate) of the transition

Gamma transitions are classified by their multipolarity order (E for electric, M for magnetic, followed by the angular momentum number l):

- E1 (Electric Dipole, l=1),

- M1 (Magnetic Dipole, l=1),

- E2 (Electric Quadrupole, l=2),

- M2 (Magnetic Quadrupole, l=2),

- up to higher orders (E3, M3, etc.).

4.5 Role of Multipolarity in γ Transitions

The multipolarity of a gamma-ray transition plays an important role in determining the behavior of nuclear decay. It affects three key aspects: selection rules, decay rates, and transition competition.

1. Selection Rules:
Gamma transitions must follow certain selection rules that conserve both total angular momentum (J) and parity (π). The change in angular momentum (ΔJ) between the initial and final nuclear states determines the possible multipolarities. For example, if a nucleus decays from a 4^+ state to a 2^+ state, then $\Delta J = 2$, and the possible multipolarities could be electric quadrupole (E2), magnetic dipole (M1), electric octupole (E3), etc., depending on whether the parity changes or remains the same.

2. Decay Rate (Transition Probability):
The transition probability, or decay rate, depends on the type of multipolarity. In general, lower multipolarity transitions occur more quickly. According to Weisskopf estimates:

- Electric dipole (E1) transitions are the fastest.

- Magnetic dipole (M1) transitions are about 100 times slower than E1.

- Electric quadrupole (E2) transitions are roughly 1000 times slower than E1.

This means that higher multipolarity transitions are less likely and take more time to occur.

3. Competition Between Transitions:
When more than one gamma-ray transition is allowed between two nuclear states, the one with the lowest multipolarity usually dominates. This is because it has the highest probability of occurring. For instance, if a nucleus goes from a 3^- state to a 2^+ state, it could do so through an E1 (electric dipole) or M2 (magnetic quadrupole) transition. Since E1 has a much higher probability, it is the most likely path.

Overall, understanding multipolarity helps predict which gamma transitions will occur and how fast they will happen.

Nuclear Detectors

We need our eyes to see and understand the world around us, but they can only see large, visible things. Tiny particles like atoms, photons, or radiation such as alpha, beta, and gamma rays are invisible to us. To observe them, we use nuclear detectors. These detectors act like a special eye that helps us see and study radiation that we can't see on our own. Some commonly used detectors are briefly discussed below.

5.1   Interaction Mechanisms

There are mainly 3 ways in which a gamma interacts with the detector crystal and deposit the energy.

1. Photoelectric Effect

2. Compton's Effect

3. Pair Production

Photoelectric Effect

If the incident gamma in contact with the detector crystal is less than 100 KeV, then it transfers all its energy to an inner-shell electron of the atom. The absorption of energy leads to ejection of an electron from the atom. Here, the ejection of electron doesn't mean complete ejection of electron from the crystal.

If E_γ is the energy which is absorbed by the atom then we can say that W is amount of energy which is used to eject an electron, and the remaining energy remains with the electron which makes it a highly energetic photoelectron $i.e., E_{e^-} = E_\gamma - W$.

Now, this ejected energetic photoelectron produces secondary electrons by interacting with neighbouring atoms or molecules and loses energy within the material by creating multiple electron hole pair along its path.

Compton's Scattering

Compton scattering is the dominant interaction mechanism for medium-energy gamma rays, typically in the range of 100 keV to 1.02 MeV. In this process, a gamma photon interacts with a loosely bound outer-shell electron in the detector crystal.

During the interaction, the gamma photon transfers only a portion of its energy E_γ to the electron, which is then knocked out of the atom. The remaining energy is retained by the photon, which scatters off in a new direction with reduced energy (E'). The amount of energy transferred to the electron depends on the scattering angle (θ). Greater scattering angles result in more energy being imparted to the electron. The formula to calculate energy of the scattered photon is given by:

$$E' = \frac{E_\gamma}{1 + \frac{E_\gamma}{m_e c^2}(1 - \cos\theta)} \tag{6.1}$$

Where:

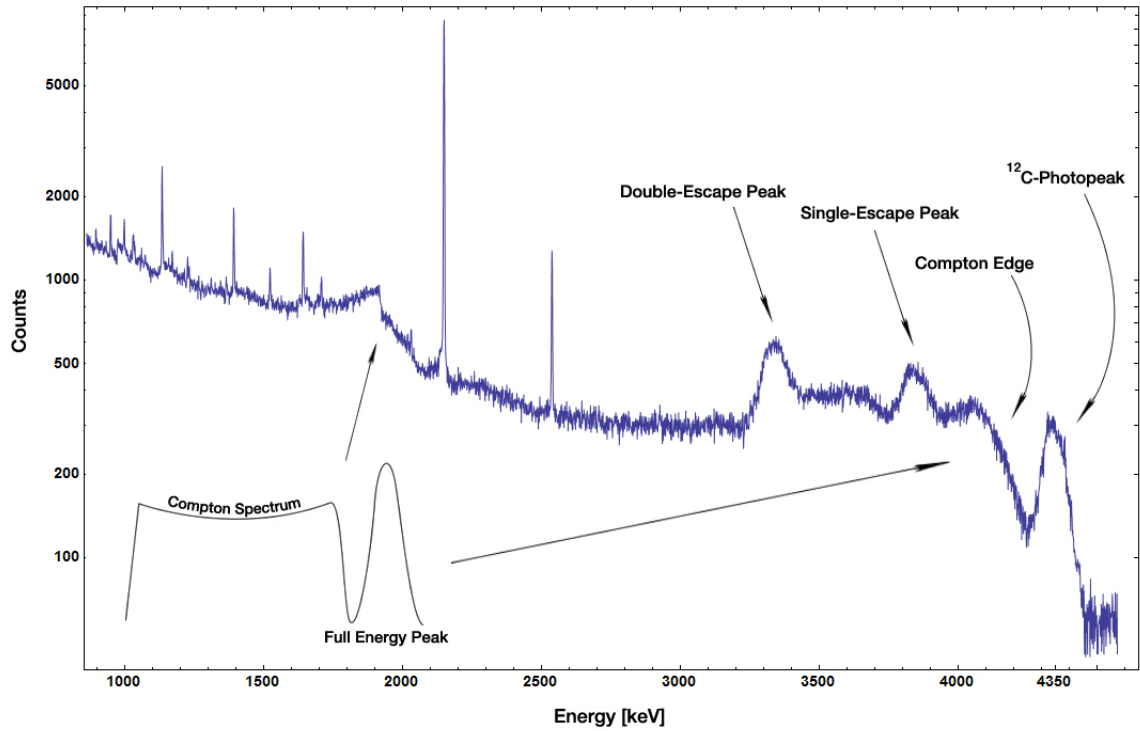E_γ is the energy of the incident photon (gamma ray)

E' is the energy of the scattered photon

E_e^{max} is the maximum energy transferred to the recoil electron (Compton edge)

m_e is the rest mass of the electron ($\approx 9.11 \times 10^{-31}$ kg)

c is the speed of light in vacuum ($\approx 3.00 \times 10^8$ m/s)

θ is the scattering angle of the photon

Figure 4: Compton Backgrounds

i) **Compton Continuum:** Gamma rays undergoing Compton scattering transfer only a portion of their energy to electrons, and the scattered photons continue in different directions with reduced energy. This results in a continuous distribution of energies being deposited in the detector, known as the Compton continuum. The continuous zig-zag pattern in the spectrum except the sharp and prominent peaks in figure (4) is Compton continuum or background.

ii) **Compton's Edge:** It is the maximum energy that can be transferred to an electron in a single Compton scattering event. When a gamma photon scatters backward (at 180°) the Compton edge appears as a distinct and sharp drop in the spectrum as shown in figure (4). Formula for maximum energy transferred to electron, E_e^{max} is obtained from equation 6.1 :

$$E_e^{\mathrm{max}} = E_\gamma - \frac{E_\gamma}{1 + \frac{2E_\gamma}{m_e c^2}} \qquad (6.2)$$

17

iii) **Back-scattering Peaks:** These are small peaks observed at lower energies in the spectrum. They occur when gamma photons are scattered outside the detector (generally from surrounding materials) and then re-enter the detector after losing some of their energy. These photons deposit only a fraction of their original energy, creating smaller peaks below the photo-peak.

Pair Production

At high gamma-ray energies (greater than 1.022 MeV), a process called pair production becomes possible. In this interaction, the gamma photon comes close to the nucleus of an atom in the detector and transforms into an electron-positron pair.

After being formed, the positron eventually encounters an electron and undergoes annihilation, resulting in the emission of two photons, each with an energy of 511 keV. These 511 KeV photons may either be fully absorbed within the detector or partially escape. If one or both of them escape without depositing their energy, it leads to the appearance of escape peaks in the energy spectrum, as shown in figure (5).
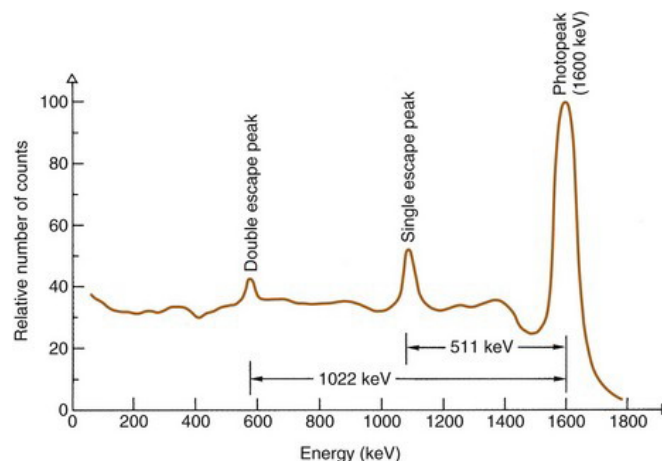
Figure 5: Escape Peaks

5.2 Scintillation Detectors

In the early 1950s, scintillation detectors played a major role in the field of gamma spectroscopy. One of the frequently used types of scintillation detectors are *thallium* doped sodium iodide scintillators *i.e., NaI(Tl)*. It allowed scientists to detect and study gamma rays using instruments that were not only effective but also small and portable [4].

What makes *NaI(Tl)* so useful is its ability to both efficiently detect gamma rays and give a reasonably clear picture of the energy they carry. Even if it was one of the earliest materials used for this purpose, they are still widely used because of their affordability and availability of large sizes.

Gamma rays don't interact directly with the detector material. They first have to transfer their energy to electrons inside the material which then lose their energy by exciting atoms in the detector crystal which gives a nearly visible blue light called as scintillation light. The detector picks up this light and converts it into a signal we can measure.

Although newer materials are available that can offer better performance in some ways, NaI(Tl) remains a reliable and widely used option for many applications where extremely high precision isn't necessary [4].

Advantages of Scintillation Detectors:

    i) High detection efficiency

    ii) Fast response time (suitable for timing applications)

    iii) Operates at room temperature

   iv) Can be manufactured in large sizes

Limitations:

    i) Lower energy resolution compared to semiconductor detectors

    ii) Light output can degrade with time or radiation damage

    iii) Requires optical coupling and dark conditions for PMT

Construction:

    i) **Scintillator Crystal:** The scintillator is the heart of the detector. It is a solid (or sometimes liquid or plastic) material that emits visible or near-visible light when struck by ionizing radiation. Common materials include:

        • **Inorganic crystals** such as Sodium Iodide activated with Thallium [NaI(Tl)], and Cesium Iodide [CsI(Tl)]

        • **Organic scintillators** such as plastics or liquids containing aromatic compounds

    The choice of material depends on the type and energy of the radiation to be detected.
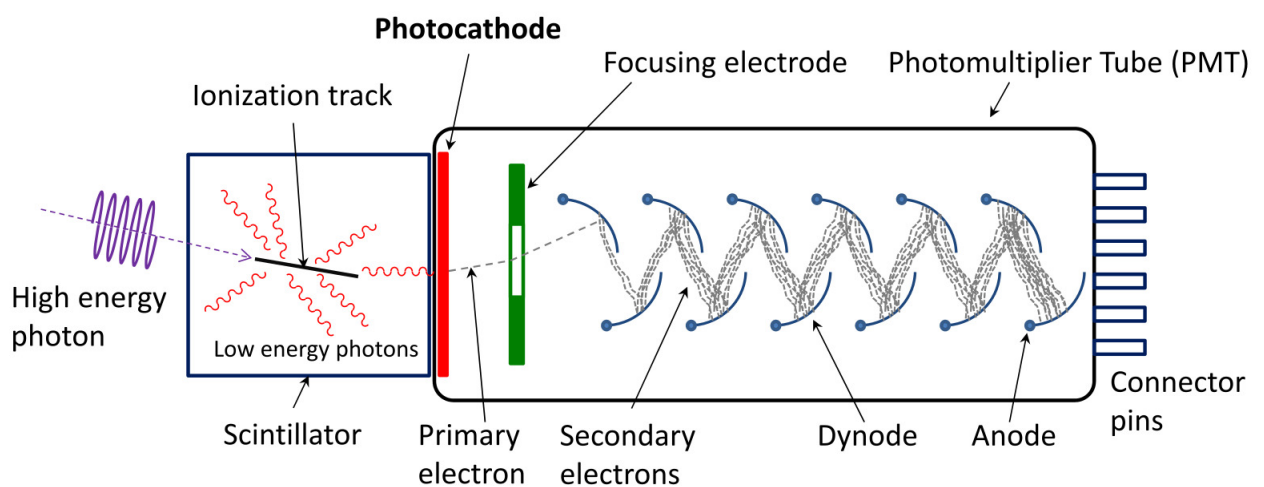
Figure 6: Scintillation Detector

ii) **Photodetector (Photomultiplier Tube - PMT):** Since the scintillation light is weak, a photodetector is used to convert it into an electrical signal. The PMT is widely used because of its high sensitivity and fast response. A PMT includes:

    (a) **A photocathode** to convert incoming light photons into electrons via the photoelectric effect

    (b) **A chain of dynodes** for successive electron multiplication

    (c) **A collecting anode** to collect the final electron cloud and produce an output signal

iii) **Optical Coupling:** To ensure efficient light transfer between the scintillator and the PMT, an optical grease or light guide is used. This minimizes light loss due to reflection or scattering at the interface.

iv) **Reflective Coating and Enclosure:** The scintillator crystal is often wrapped with a reflective material such as Teflon or aluminum foil to redirect escaped photons back into the crystal. The entire assembly is enclosed in a light-tight housing to shield the PMT from external light sources and prevent interference.

Pulse Generation:

When gamma rays or other ionizing radiation interact with the scintillating crystal (refer to Section 5.1 for interaction types such as photoelectric effect, Compton scattering, and pair production), they deposit energy within the material, exciting the atoms or molecules of the scintillator.

As these excited states return to their ground states, they emit light in the form of visible or near-visible photons—this is called scintillation light. This light is then used to generate an electrical signal through the following process:

i) **Photon Generation:**
The gamma-ray interaction produces a burst of scintillation photons inside the crystal as shown in fig.7. The number of photons is directly proportional to the energy deposited by the incident radiation.

ii) **Light Collection:**
These scintillation photons travel through the crystal and are directed toward the photodetector, usually a Photomultiplier Tube (PMT), using optical coupling material to maximize transfer efficiency.

iii) **Photon-to-Electron Conversion (Photocathode):**
When the scintillation light reaches the photocathode of the PMT, photoelectrons are emitted due to the photoelectric effect. However, not all photons contribute—only a fraction (typically 20–30%) produce photoelectrons, based on the quantum efficiency of the photocathode material.

iv) **Electron Multiplication (Dynode Chain):**
The emitted photoelectrons are accelerated toward a series of dynodes. At each dynode, one incoming electron releases multiple secondary electrons. This chain reaction of electron multiplication continues over several dynode stages, usually 8 to 12.
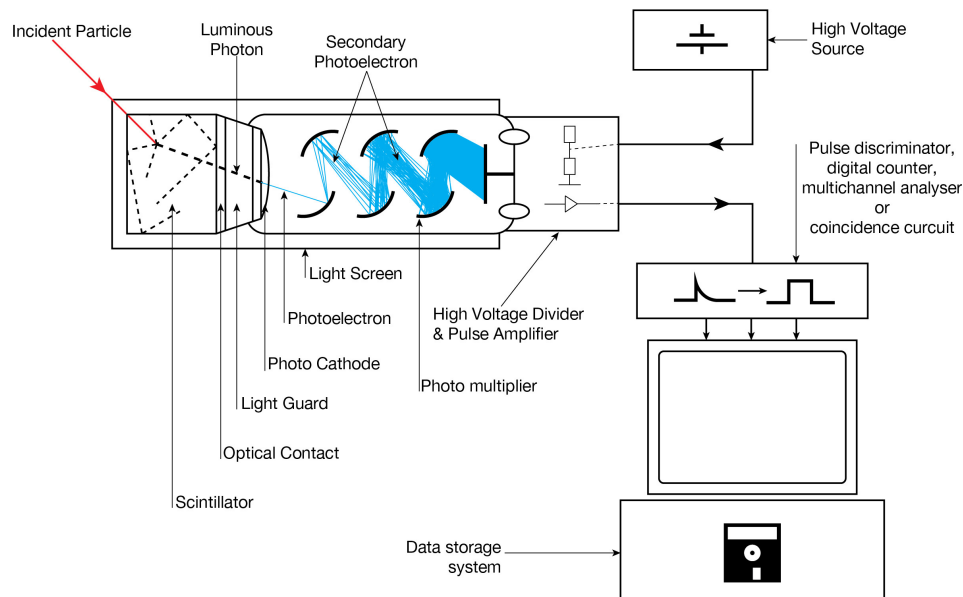
Figure 7: Scintillation Detector

v) **Pulse Formation (Anode):**
   The large number of secondary electrons produced is collected at the anode of the PMT. This collection results in a fast and measurable electrical current pulse. The height of this pulse is proportional to the original energy deposited by the radiation.

5.3   Semiconductor Detectors

When the gamma ray interacts with detector crystal, using the energy it produces information carriers or photoelectrons. The energy required to produce a single pair of information carriers is in the order of 100 eV. The information carriers produced by interaction with gamma ray is only a few thousands in other detectors. Here, Statistical fluctuation is so small that it has an inherent limitation on energy resolution under the best circumstances, and nothing could be done to improve the resolution beyond this point.

The only way to increase the no. of information carriers per pulse is by using semiconductor crystal instead of scintillation crystal in a detector. The early versions were indeed able to provide better resolutions and were called **"Crystal Counters"**. Now, it's commonly referred as semiconductor or solid-state detectors. The term **"Solid-state"** refers to devices that are based on collecting electron hole pairs from semiconductor media [4].

Advantages of Semiconductor Detectors:

- Better energy resolution

- Comparatively smaller in size as compared to traditional detectors.

- Relatively fast timing characteristics

Drawbacks:

- Small sizes

21

- High susceptibility to performance degradation from radiation induced damage

Construction:

i) **Semiconductor Material:** The construction of a semiconductor detector is centred around a single crystal of semiconductor material, most commonly **High-Purity Germanium (HPGe)** or **Silicon (Si)**. These detectors are typically designed as large-area p-n junction diodes, or more precisely, p-i-n structures where an intrinsic (undoped) region is sandwiched between p-type and n-type layers. This intrinsic region forms the active detection volume, which is made as large as possible to increase the detector's efficiency for gamma-ray interactions.

There are three main regions:

(a) **P-type region:** Doped with acceptor impurities (positive holes dominate)

(b) **N-type region:** Doped with donor impurities (electrons dominate).

(c) **Intrinsic (i-type) region:** Very lightly doped or undoped—this is the active volume where most interactions occur.

ii) **Depletion Region:** Different semiconductor detectors require varying amounts of energy to generate free charge carriers. For example, *germanium (Ge)* requires approximately **2.9 eV**, while *silicon (Si)* requires around **3.6 eV** to produce a single electron-hole pair.

When a reverse bias voltage is applied across the p-n junction, it creates a depletion region where free charge carriers (electrons and holes) are swept out. This region becomes highly sensitive to incident radiation. In detectors like HPGe, the entire crystal is often fully depleted to maximize the volume available for detection, see figure (8). (Refer to section 5.1 to know about γ - interaction mechanism.)
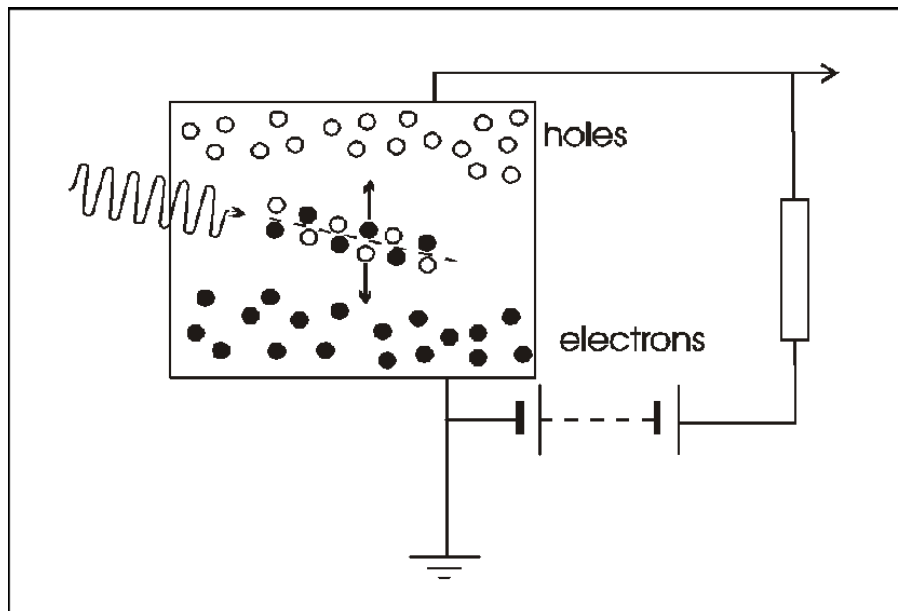

Figure 8: Semiconductor Detector

iii) **Collecting Electrodes:** Thin metal contacts (often *aluminium* or *gold*) are deposited on the top and bottom surfaces of the crystal where one acts as the cathode (negative terminal) and the other as the anode (positive terminal). These allow for application of

the reverse bias voltage and collection of charge carriers (electrons and holes) generated by incoming radiation.

iv) **Cryogenic Liquid:** In the case of **germanium detectors**, due to their low band gap energy (0.67 eV), thermal noise becomes a significant issue at room temperature. To reduce this noise, Ge detectors must be operated at very low temperatures—usually around 77 K—using a liquid nitrogen cryostat. In contrast, **silicon detectors**, which have a higher band gap (1.1 eV), can often operate at or near room temperature for low-energy radiation applications.

v) **Pre-amplifier:** The preamplifier is used as a charge sensitive integrator. It uses a *"Field Effect Transistor (FET)"* because the output signal from the detector is of very high impedance. If we use a low impedance device then it will draw current and degrade the signal resolution. Also, it is placed as close as possible to the detector to minimize noise and signal degradation during transmission.

vi) **Amplifier:** After the signal is processed through preamplifier, amplifier is mainly used to shape the stable signal and amplify it.

vii) **Multi Channel Analyser (MCA):** MCA is vital for recording the pulse counts and their respective amplitudes (which is converted to a channel). They also do sorting of the pulse information arrange them in proper order and create a histogram corresponding to these events during a single gamma detection.

viii) **Encapsulation of Components:** The entire assembly, including the detector crystal, electrodes, and cooling system (if needed), is enclosed in a vacuum-tight housing with a thin entrance window that allows gamma rays to enter while minimizing absorption. Additional radiation shielding (such as *lead* or *copper*) may surround the housing to minimize background interference.

Pulse Generation:

The movement of charge carriers induces a weak current pulse in the external circuit i.e., pre-amplifier, amplifier, MCA etc. as shown in fig. (9).
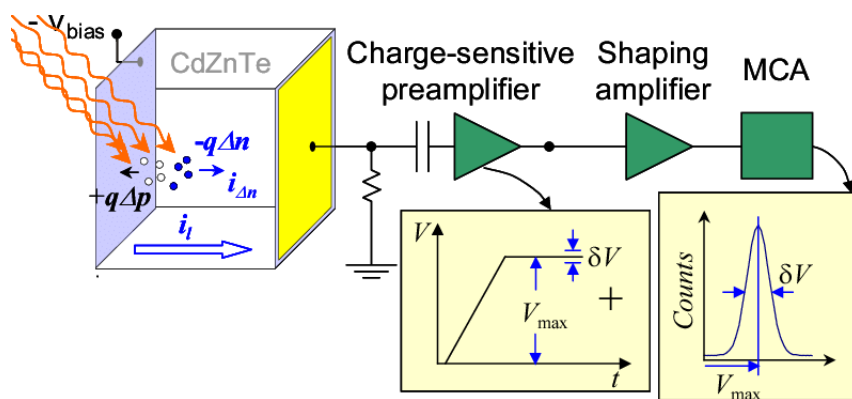
Figure 9: Pulse processing through pre-amplifier to multi channel analyser

Characteristics of the output signal:

i) **Small amplitude**

ii) **The signal has high impedance output**

iii) **They are susceptible to electronic noise**

iv) **Very short duration current pulses**

To use this weak current signal the collecting electrodes acts as a bridge between the detector and the preamplifier. The cathode is connected to ground and anode is connected to the input of the preamplifier using a co-axial cable.

The preamplifier integrates the current pulse with respect to time to get voltage pulse. This voltage pulse is proportional to charge deposited (*i.e., energy deposited by γ ray*). This output voltage pulse has long decay time constant (generally 50-100 μs.

The voltage pulse is further amplified through the shaping amplifier. This process is relatively easier as compared to the pre-amplifying step because the output pulse is stable. Generally, these amplifiers are designed to take high impedance input and give low impedance output.

5.4   Spectrum Formation

What we need, to understand a specific nuclear source is a spectra. However, we only get an amplified voltage pulse from the rest of the detector. Therefore, a **MCA** (Multi Channel Analyser) plays a vital role to convert each pulse into a radiation event which is stored in the form a histogram (*spectra*).But how...?

Each pulse's amplitude is proportional to the energy deposited in the detector and this pulse is an analog signal. So, MCA converts it to a digital signal using **ADC** (Analog to Digital Converter). This also results in amplitude being converted to a digital value. And this digital value corresponds to a channel in MCA's memory. Generally we call these channels as *ADC channels*.

Similarly, MCA assigns different type of pulses to an unique channel no. and they are alsways in ascending order. *For example, lower energy pulse gets lower channel and higher energy pulse gets higher channel.*

As pulses continue to arrive, the MCA increments the counts in appropriate channel for each event. Hence we get this spectra where *x-axis* corresponds ADC channels and *y-axis* corresponds to the counts. What's fascinating about MCA is that it also records the count of each pulse which is crucial for studying the graph or spectra.

Standard Isotope Sources:

We know that channel no.s of visible peaks belong to a specific γ, but not their relation *i.e., which channel belongs to which γ*. To establish this relationship, we perform energy calibration using a radioactive isotope source with known energy levels. This process involves determining calibration parameters (A, B, and C) that allow us to convert channel numbers into energy values without repeatedly plotting graphs.

Uncalibrated Spectra:

As previously stated, digital counters record all detected gamma-ray events, storing channel numbers (*x*-axis) and their corresponding counts (*y*-axis). This raw data is saved as an event file. To generate an uncalibrated spectrum, we process this file using **BINDAS** (Basic Nuclear Data Analysis Software). The installation and use manual has been attached as a reference [8].

An uncalibrated spectrum is generated from the raw event file, where channel numbers and counts are recorded but not yet mapped to energy levels. Using BINDAS, we convert the event data into a spectrum file, which remains uncalibrated until energy calibration is performed. An uncalibrated spectra of ^{152}Eu is shown in figure (10).

**Figure 10:** Uncalibrated Spectra of ^{152}Eu

Shape of the Spectra Peaks:

Gamma-ray spectra are characterized by distinct peaks that represent discrete energy emissions from radioactive sources. These peaks usually follow a bell-shaped curve, closely approximating a Gaussian (normal) distribution. The overall shape and characteristics of these peaks carry valuable information about the radiation source and the performance of the detector system.

Why Spectral Peaks are Bell-Shaped?

- **Quantum Mechanical Effects:** The interaction of gamma rays with matter involves stochastic processes, leading to slight variations in the energy deposited in the detector. Even if a gamma-ray source emits photons of identical energy, the actual recorded energy can vary slightly due to these random fluctuations.

- **Detector Resolution Limitations:** No detector can measure energy with perfect precision. Instead, the energy is spread over several channels, forming a distribution. The detector's ability to sharply resolve energy levels defines the width and clarity of the peak.

Example: The 1408 keV peak from Eu-152 (as shown in Fig.11) is a typical example of a Gaussian-shaped spectral peak observed in well-calibrated detectors.
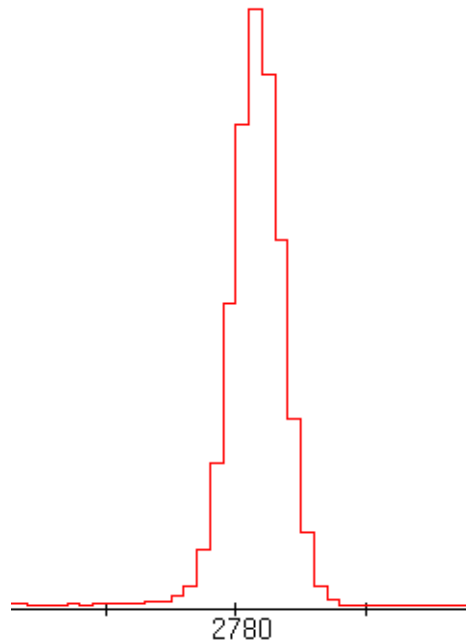
**Figure 11:** 1408 KeV Energy Peak of ^{152}Eu Spectra

5.5 Characteristics of Spectral Peaks

Understanding spectral peak features is essential for qualitative and quantitative gamma spectroscopy. The following characteristics are used for peak identification, source activity estimation, and efficiency calibration.

i) **Peak Height:** It represents the maximum count rate at the centroid of the peak. It visually indicates how intense or strong a particular gamma-ray emission is at that specific energy.

ii) **Peak Centroid:** The centroid refers to the channel number or energy value at the center of the peak, which corresponds to the most probable energy deposited by the gamma ray or the energy expectation value of the gamma.

iii) **Peak Width – Full Width at Half Maximum (FWHM):** The FWHM describes the width of the peak at half of its maximum height. It is a crucial measure of the energy resolution of the detector. Fig.12 and fig.13 shows the differences between spectras produced from semiconductor detector and scintillator respectively.

iv) **Peak Area:** The area under the spectral peak is directly proportional to the number of gamma rays detected at that energy. It is obtained by summing the counts across the channels that define the peak.

Importance:-

(a) **Source Activity Estimation:** Peak area, combined with efficiency and measurement time, is used to calculate the activity of a radioactive sample.

(b) **Efficiency Calibration:** Comparing peak areas of known standards helps build efficiency curves.

26
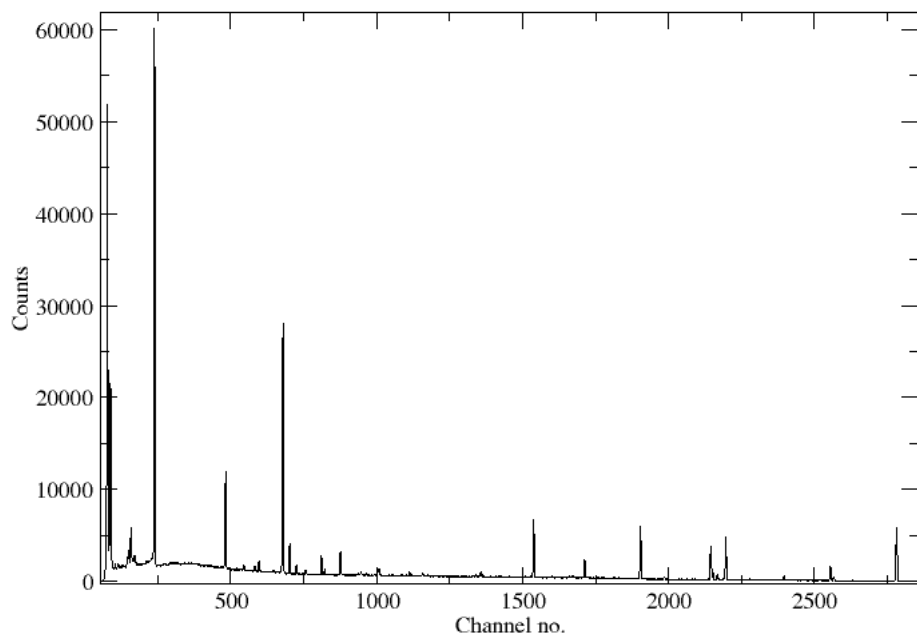
Figure 12: Spectra of ^{152}Eu from HPGe Detector
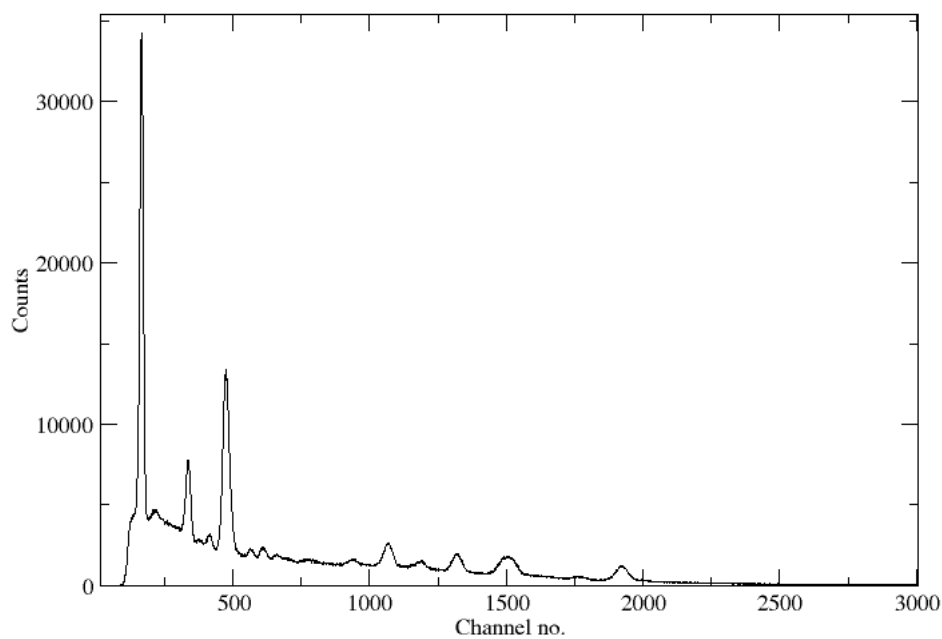
Figure 13: Spectra of ^{152}Eu from Scintillation Detector

Spectrum Analysis

The most commonly used reference source for energy calibration is ^{152}Eu (Europium, as its gamma-ray energies are well-documented). And the gamma rays are detected using the exact same detector which is going to detect the gamma ray from unknown radio active source (*here* ^{115}In). This way we are able to know the unknown energy levels of a nucleus using a known one. By analyzing its spectrum, we obtain the necessary calibration parameters, which can later be applied to spectra from unknown radioactive sources.

6.1 Energy Calibration

To perform energy calibration, we begin by identifying prominent peaks in the gamma spectrum, typically using a known calibration source such as ^{152}Eu. The peak centroids are determined using the `gf3` fitting tool in RadWare [3], which fits Gaussian functions (with optional polynomial background) to accurately extract the channel number corresponding to each gamma energy. `Gf3` also outputs the FWHM and area for each peak, which are later used for resolution and efficiency analysis. Otherwise, we can also use python code for getting calibration parameters [9].
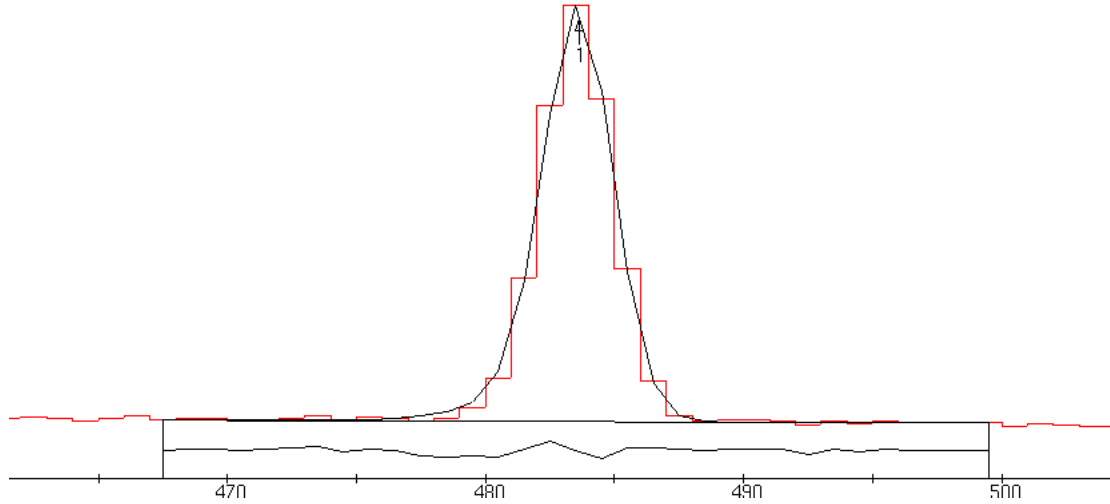
Figure 14: Gaussian fitting of 244 KeV Energy peak of ^{152}Eu

The known gamma energies as are known through **ENSDF** (*Evaluated Nuclear Structure Data File*) [1]. Once several known peaks are fitted, we plot the corresponding channel numbers (x-axis) against their known gamma energies (y-axis). A second-order polynomial of the form:

$$Y = A + BX + CX^2$$

is fitted to this data to generate the calibration curve. The coefficients *A*, *B*, and *C* are the calibration parameters.One of the easiest ways to do this is using **"Polynomial Regression Data Fit"** [7] or using the python code here [9]. Once this equation is established, it allows conversion of any channel number in the spectrum to its corresponding energy value, enabling full-spectrum calibration.

Creation of Calibrated Parameters File:

Once multiple X and Y value is listed, using polynomial regression we get the values of 3 co-efficients which is also considered as calibration parameter for that particular spectra. Here is an example of calibration parameter *i.e., A, B and C values* of 1st spectra of ^{152}Eu:

$$0.20567144865662518 \qquad 0.5062541066702939 \qquad -1.0535333243732104 \times 10^{-8}$$

Calibration parameters of all the spectra of the spectrum or spk file is listed in text file in `.cal` format with tab or equal spacing between them. This file is known as Calibration parameters file and often follow this pattern (e.g., `Calibration_parameters.cal`). The parameters obtained for each detectors and their respective crystal is shown in the following table (1).

Table 1: Calibration Parameters for Detectors and Crystals

| S.No.	Detector	Crystal	A	B	C
1		C1	0.20567144865662518	0.5062541066702939	-1.0535333243732104e-08
2	D1	C2	0.1825674882187084	0.5001084182412545	8.586675007361628e-09
3		C3	0.21273534358455076	0.5006858494759179	-1.2522235954755059e-08
4		C4	0.170758605326151	0.4991516614444606	1.4942367199022554e-08
5		C1	0.207444302259794	0.497547453485133	-3.7471160513792845e-08
6	D2	C2	0.216383714198259	0.4976753968995047	-1.6738943665470125e-08
7		C3	0.15718740730562786	0.500448196042998	-2.1539224870565614e-08
8		C4	0.199587889174154	0.4999622424926401	-2.8493561089115747e-08
9		C1	0.268221297328481	0.4969324127929313	1.5291973824645566e-08
10	D3	C2	0.211877585388796	0.500456177918646	-3.2335663567894183e-09
11		C3	0.169185291644998	0.4997287405074681	-4.9194249506176063e-08
12		C4	0.339648966236102	0.5007096582052	1.9474567454274614e-08
13		C1	0.30219307383443	0.502754192945859	-7.73764837583845e-08
14	D4	C2	0.258049716650045	0.5017871558881493	-3.179586679859598e-08
15		C3	0.312004007662044	0.5023741836118149	1.1033956280166382e-08
16		C4	0.2584240063858398	0.5006720688897939	-2.4404297698050592e-08
17		C1	0	0	0
18	D5	C2	0.365494131340331	0.5058077404557514	6.945632550565584e-08
19		C3	0	0	0
20		C4	0.27736399619268803	0.5052000262758443	2.2663161484104152e-08
21		C1	0.30306026779971346	0.5055474358928178	2.7628120471817174e-08
22	D6	C2	0.227200591611345	0.5008193280597192	2.6594858786846024e-08
23		C3	0.08601600075095403	0.5049385841050569	-2.651601490934787e-08

S.No.	Detector	Crystal	A	B	C
24		C4	0.20450493224041655	0.5006130985533725	4.136731523323591e-08
25		C1	0.2973473820357825	0.4988201017255926	-1.2904125616278952e-08
26	D7	C2	0.20053495957077863	0.5031414296937043	2.9152363836698405e-09
27		C3	0.1880925171878761	0.5017239707165672	-4.649396617010751e-09
28		C4	0.28738559154123505	0.5026311573527671	5.8617057802029924e-08
29		C1	0.08182035016485012	0.5004122443566328	1.5405017468924646e-09
30	D8	C2	0.26089644633346015	0.5024999096515073	2.949615747821247e-08
31		C3	0.21309964545681367	0.5019602739957616	4.789164217307748e-08
32		C4	0.22457828048874434	0.5074559052698371	-1.3823841008666523e-08
33		C1	0.9416582290832923	0.7235226022219173	4.4004671052780064e-06
34	D9	C2	0	0	0
35		C3	0	0	0
36		C4	0	0	0
37		C1	0.02388935644504224	1.234241011631255	6.5616009990491964e-06
38	D10	C2	0	0	0
39		C3	0	0	0
40		C4	0	0	0
41		C1	-0.26630888001512776	1.0535093533276034	4.605548291658886e-06
42	D11	C2	0	0	0
43		C3	0	0	0
44		C4	0	0	0
45		C1	1.6220571904759034	0.5634735674162378	2.459632956052062e-06
46	D12	C2	0	0	0
47		C3	0	0	0
48		C4	0	0	0
49		C1	3.193277287784258e-08	1.8309931828106294	-1.809175009555335e-13
50	D13	C2	0	0	0
51		C3	0	0	0
52		C4	0	0	0
53		C1	2.478764155513156	1.215809026219021	1.2538741575925654e-05
54	D14	C2	0	0	0
55		C3	0	0	0
56		C4	0	0	0
57		C1	0.3752733845467286	1.2958247192837709	6.7530507647236375e-06
58	D15	C2	0	0	0

S.No.	Detector	Crystal	A	B	C
59		C3	0	0	0
60		C4	0	0	0
61		C1	0.4584107680711713	1.9055779659675225	7.022435279739306e-06
62	D16	C2	0	0	0
63		C3	0	0	0
64		C4	0	0	0
65		C1	1.0987447721901005	0.8742390931903715	4.744422234954019e-06
66	D17	C2	0	0	0
67		C3	0	0	0
68		C4	0	0	0
69		C1	1.2373394116459024	1.5321795827810678	1.429921531656475e-05
70	D18	C2	0	0	0
71		C3	0	0	0
72		C4	0	0	0

Calibrated Spectrum Formation:

The event file was calibrated using the BINDAS software with the derived calibration parameters. The resulting calibrated spectrum was used to verify the calibration accuracy. Fig. 15 shows the energy-calibrated γ-ray spectrum, where channel numbers have been converted to their corresponding energy values. Characteristic peaks from the [152]Eu calibration source appear at their expected energies (344.2 keV, 778.8 keV, etc.), confirming the accuracy of the energy calibration across the measured range.
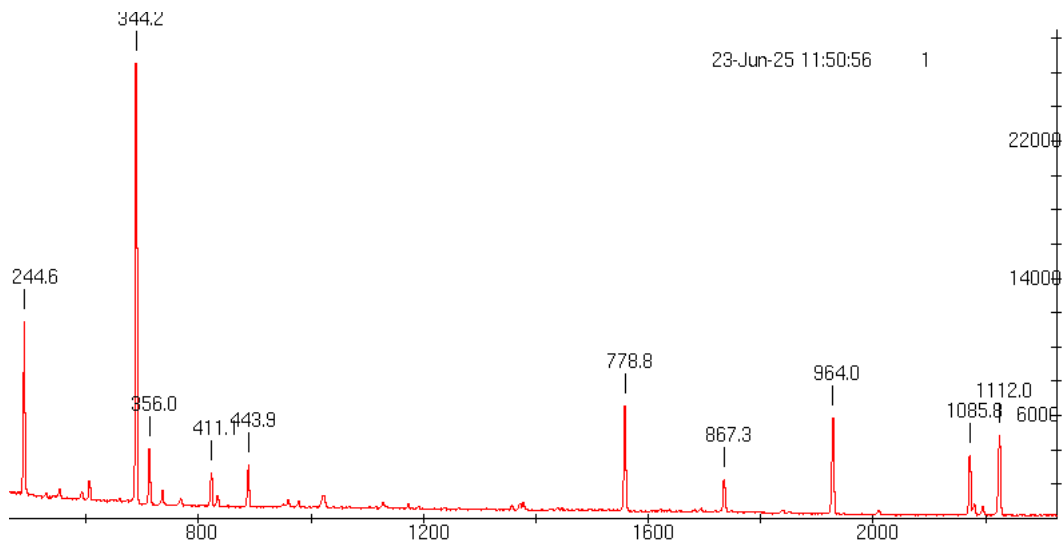
Figure 15: Calibrated Spectra of ^{152}Eu

31

Calibration Accuracy Verification:

To ensure the accuracy of the energy calibration, spectra acquired under different conditions or at different times are overlaid using RadWare. Any visible shift in peak positions between these spectra indicates a calibration drift or instability in detector electronics.

By comparing multiple spectra visually and numerically, especially those of standard sources, we confirm the consistency of the centroid positions. Peaks should remain within ±1 channel of their calibrated positions to be considered stable. This verification step is crucial before proceeding with further analysis like gating or matrix generation.
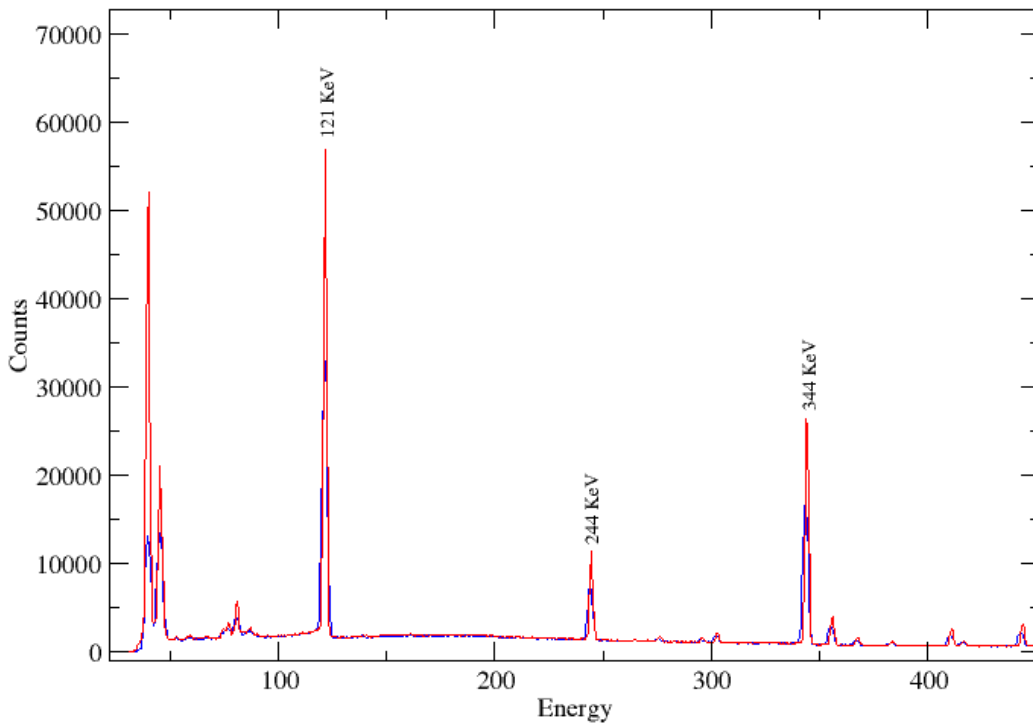
Figure 16: Spectra Overlay of 3 spectras from ^{152}Eu

6.2   Spectrum Matrix Construction

Using the `xmesc` module in RadWare [8], we construct a two-dimensional gamma-gamma coincidence matrix from the list-mode data acquired during the experiment. This module is particularly designed to process event-by-event data files generated from HPGe detector arrays. In our case, the data were collected in list-mode format, where each event records energy deposits in multiple detectors along with their time correlations.

The `xmesc` utility reads these time-correlated events and constructs a matrix in which the X and Y axes represent the energies detected in two coincident gamma detectors. Each entry in the matrix corresponds to a pair of gamma rays detected in prompt coincidence, allowing us to identify cascade transitions between nuclear states.

This matrix is then used to generate:

- **Projection spectra:** Energy spectra projected from one axis to study gamma intensities regardless of coincidence. We obtain a total of 2 projections. One from the X-axis (in fig.17) and another from Y-axis. Generally, we use X-axis projection to find the coincidence gamma energy levels from the spectrum.

  The generation of gated spectra is entirely dependent on projection spectra. Because in case if there are two nuclei who are decaying together it will be still visible, even after applying gate we will still get the gated energy.
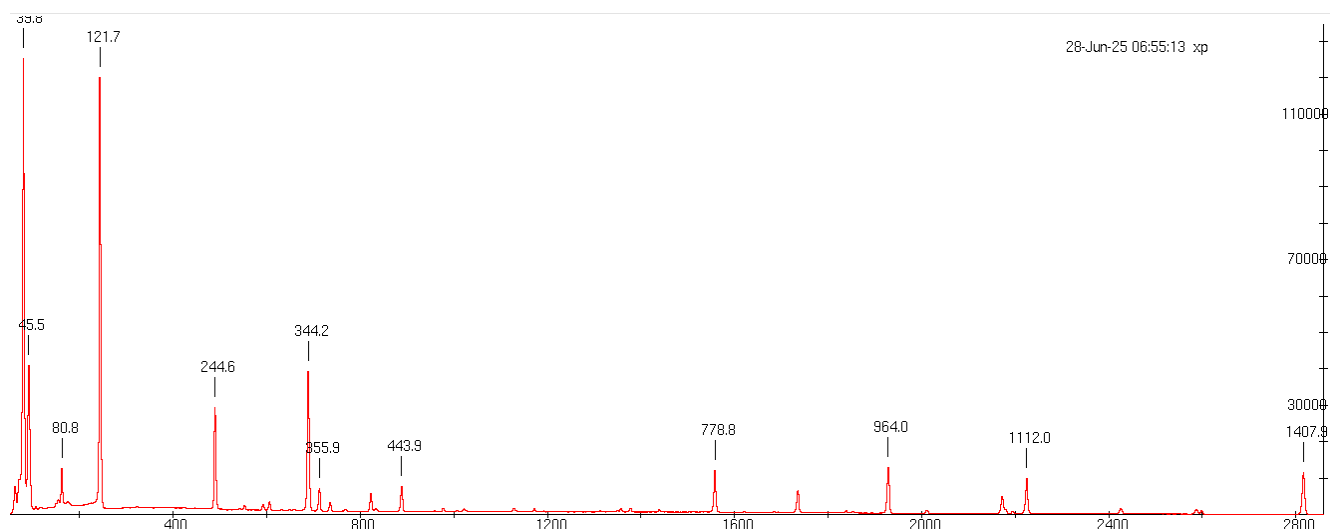
Figure 17: X-axis Projection Spectra

- **Background spectra:** Created and subtracted using sideband techniques within xmesc, allowing clearer identification of true coincident events as shown in fig.18.
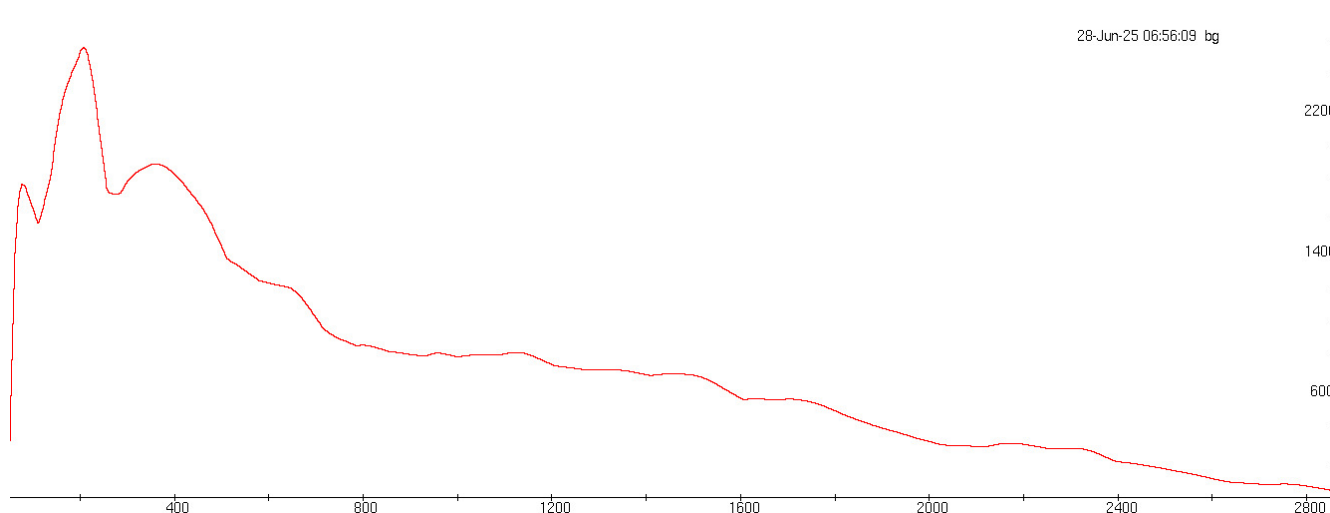
Figure 18: Background Spectra

Such matrix construction is vital in analyzing multi-gamma decay schemes and identifying cascade relationships.

6.3 Generation of Gated Spectra

Gated spectra are produced by setting an energy gate around a specific peak in the coincidence matrix. This isolates events where a gamma ray of known energy is detected in coincidence with another gamma ray.

In `xmesc`, gates are applied to eliminate background and enhance spectral features corresponding to true coincidences. This process:

- Highlights cascade gamma transitions.

- Helps distinguish coincident and non-coincident gamma emissions.

- Aids in constructing level schemes for the parent nucleus.
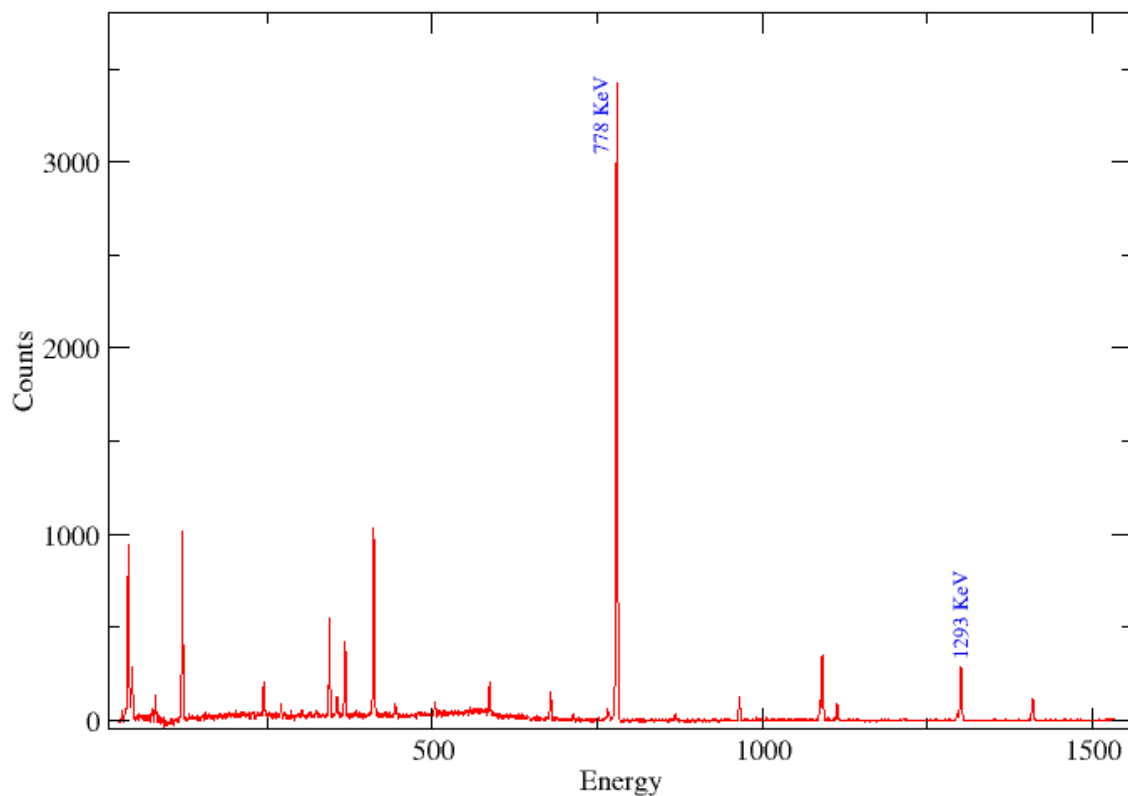
Figure 19: Gated Spectra of 344 KeV

Gated spectra are especially useful in resolving overlapping peaks or weak transitions obscured in the full projection.
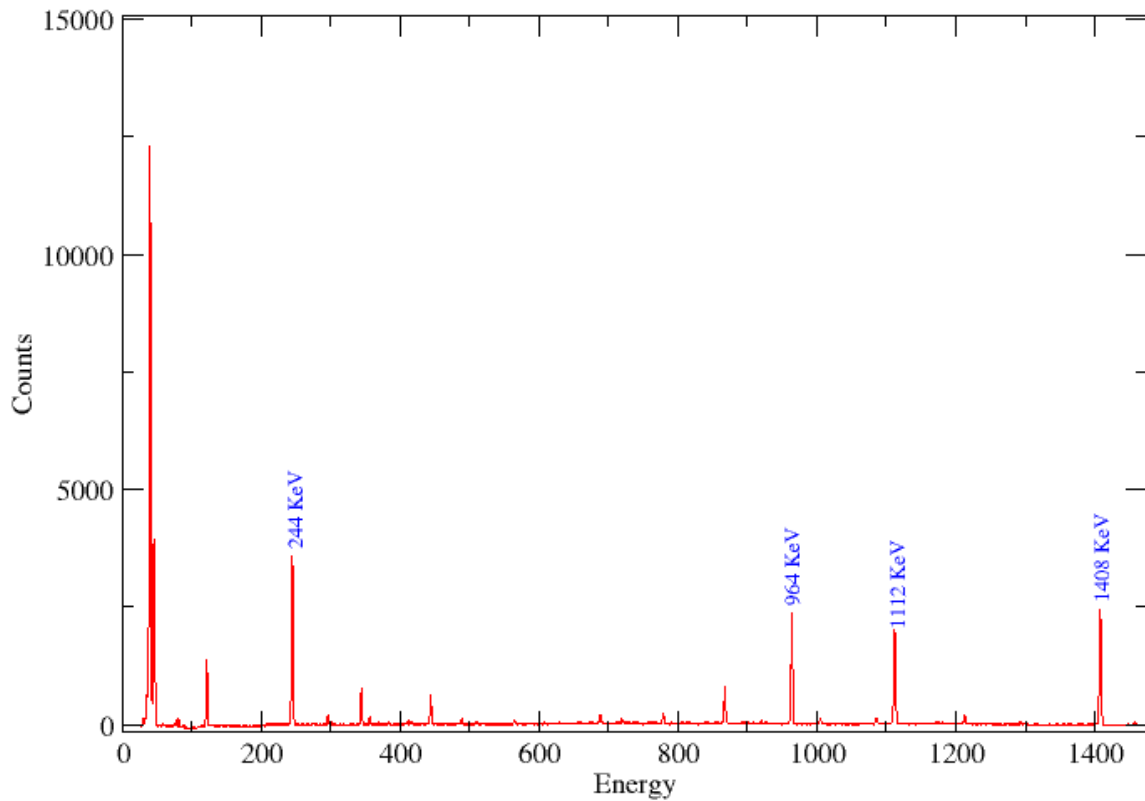
Figure 20: Gated spectra of 121 kev gamma of ^{152}Eu

6.4 Addback Spectra Formation

For Clover detectors, each detector head consists of four high-purity germanium crystals. Instead of analyzing them separately, we improve detection efficiency and photopeak count rates by summing the energy deposited across all four crystals — a process called **addback**.

Using RadWare, individual spectra from the four crystals are combined to generate an addback spectrum for each Clover detector. This process:

- Enhances the full-energy peak efficiency.

- Reduces Compton background.

- Improves peak-to-total ratio, especially in high-multiplicity events.

Addback spectra are essential in studies involving weak transitions or requiring high gamma detection efficiency.

Spectral Analysis ^{116}In

The study of nuclear reactions involving neutron capture provides valuable information about the structure and energy levels of atomic nuclei. One such important reaction is ^{115}In$(n, \gamma)^{116}$In, in which a thermal or epithermal neutron is absorbed by a stable indium nucleus, producing an excited ^{116}In nucleus. This excited nucleus quickly de-excites by emitting a series of prompt gamma rays, which carry energy signatures of the internal nuclear transitions.

In this work, calibration is performed using a standard radioactive source, ^{152}Eu, which emits gamma rays of known energies. These known peaks serve as reference points for building a relationship between the channel number and energy. A second-degree polynomial function is fitted to this data to obtain calibration parameters. Once the calibration is complete, it becomes possible to convert the unknown gamma peaks from the ^{115}In(n, γ) spectrum into actual energy values.

7.1 Spectra Creation

To analyse different aspects of the the nuclear decay we need the spectrum file. But previously we only needed a single spectrum file because it was for calibration parameters only. Now, we will do multiple runs for our main nuclei which will be studied *i.e.,* ^{116}In. If we will convert each file one by one then it will be very time consuming. So, we will create a script file for multiple runs for example; 5 or 10 events files can be converted into .spk format one after another. The script format file is provided in the appendix [9-D] and reference [8]. As an example, 1st spectra of 1st spectrum file from ^{116}In is shown in fig.21.
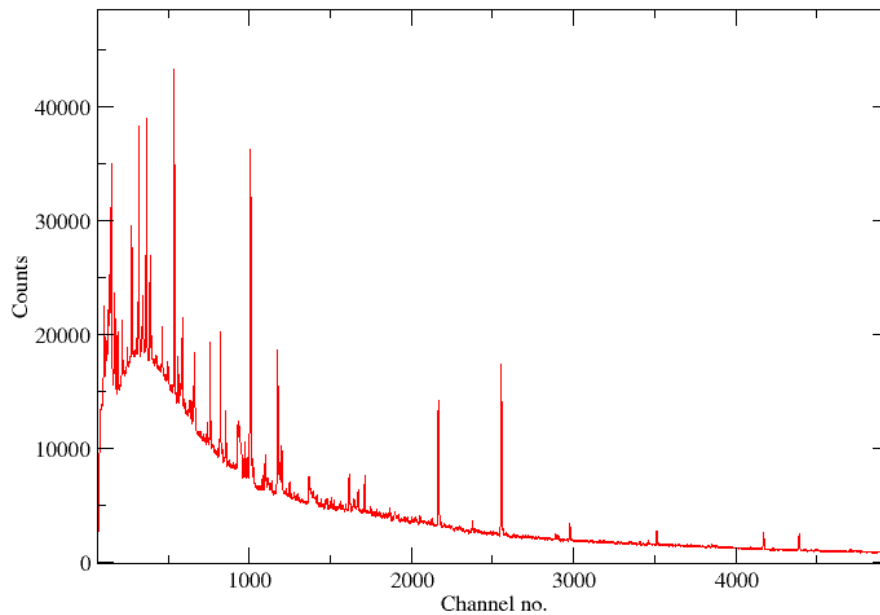
Figure 21: 1st spectra of ^{116} In

7.2 Calibrating Spectra using ^{152}Eu parameters

Eventhough, we created the uncalibrated spectras first, the most important step after getting the calibration parameters is to calibrate the event files using the parameters. Similarly, like spectra creation we will do a script run for the calibration as well and the format has been given in the appendix [9-A]. The calibrated spectras are shown in fig.22 and fig.23. Now, we will check the spectras by overlaying one atop other and see if there is an peak mismatch or shift. If there is any mismatch we will note down the no.s of spectras of every single spectrum file (i.e., .spk file). Multiple files can be calibrated at a time using this script in appendix [9-C].
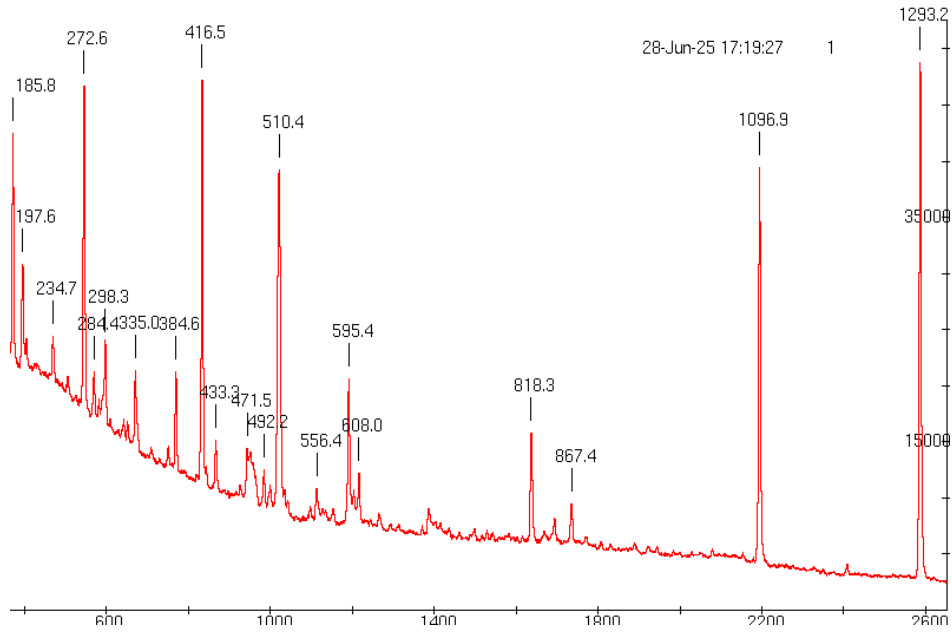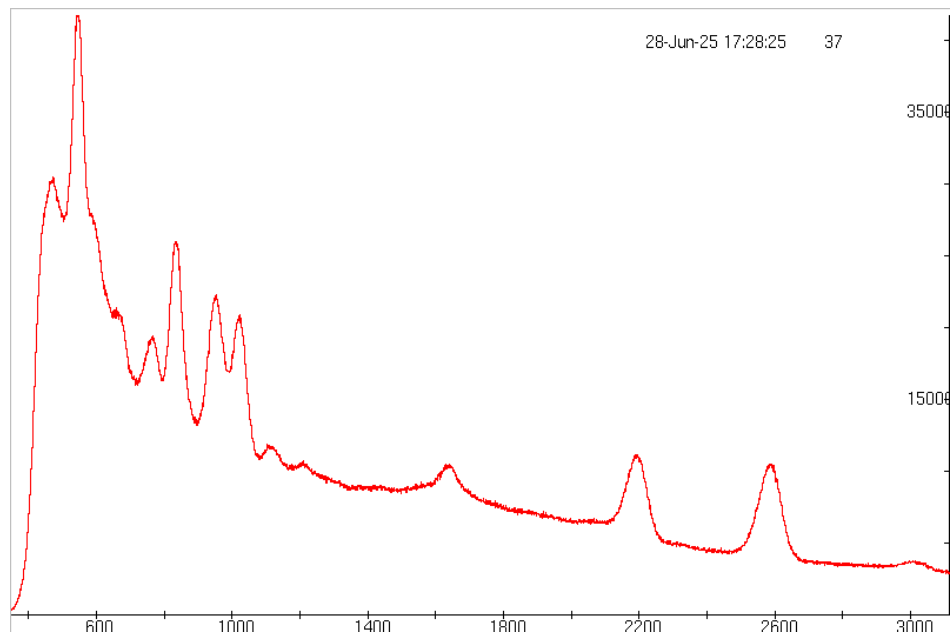

Figure 22: calibrated Spectra of ^{116}In

Figure 23: 37th calibrated Spectra of ^{116}In

7.3   Re-calibrating the peak shifted spectra

We will take the centroid data of spectras with noticeable peak shift to re-calibrate the spectrum as X and energy value from **ENSDF** [1] as Y. After we obtain the calibration parameters for a single spectrum file of ^{116}In, we will use that data in the other spectrum files. By doing this we can calibrate a large no.s of spectrum files without calibrating each and every spectrum which will save a lot of valuable time. Now, we will also match the energy of the spectras with those from **ENSDF** to verify that our energy values are accurate if the error is within 0.3KeV.
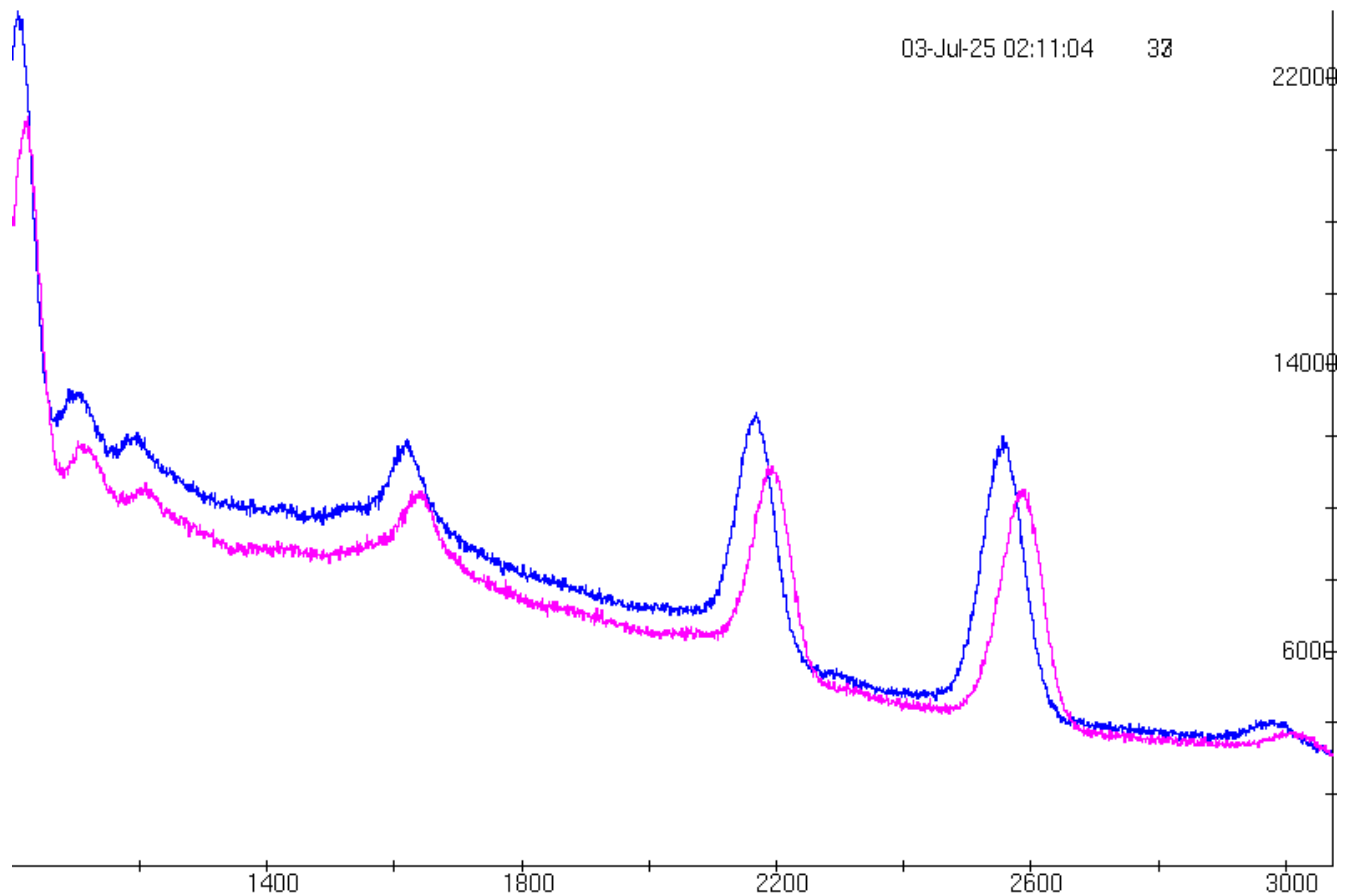
Figure 24: Peak Shifted Spectra

These peak shifts usually occur because the digitizers run continuously for long periods during experiments. Over time, the increase in temperature can cause a shift in voltage gain, which leads to a displacement of peaks in the energy spectrum.

So, after recalibration there will be no peak shift which will ensure that our calibration remains accurate for other files.
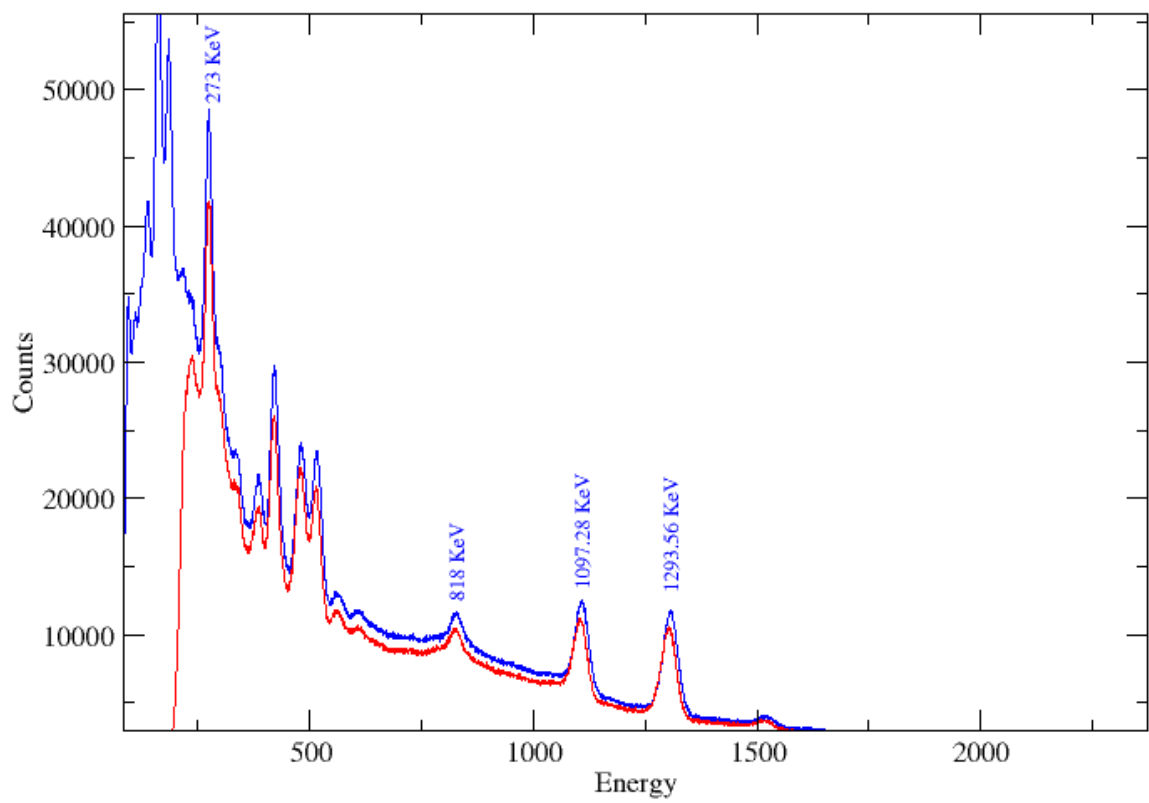
Figure 25: Spectra Overlay after recalibration

7.4 Matrix Formation

Using the matrix creation script (Appendix 9-B), we generate a two-dimensional (2×2) $\gamma - \gamma$ coincidence matrix. This matrix is constructed by sorting the list-mode event data into a histogram, where both axes represent gamma-ray energies detected in coincidence. From this matrix, we can extract the projection spectra by projecting the matrix onto one of the energy axes, which provides the overall energy distribution of coincident events. Additionally, background spectra can be obtained using sideband gating or random gate regions to account for non-coincident or accidental events.

Furthermore, by applying energy gates on specific known gamma-ray peaks within the matrix, we can isolate coincident transitions and generate various gated spectra of ^{116}In. These gated spectra are crucial for identifying gamma cascades and studying the nuclear energy levels and decay schemes of the isotope in detail.
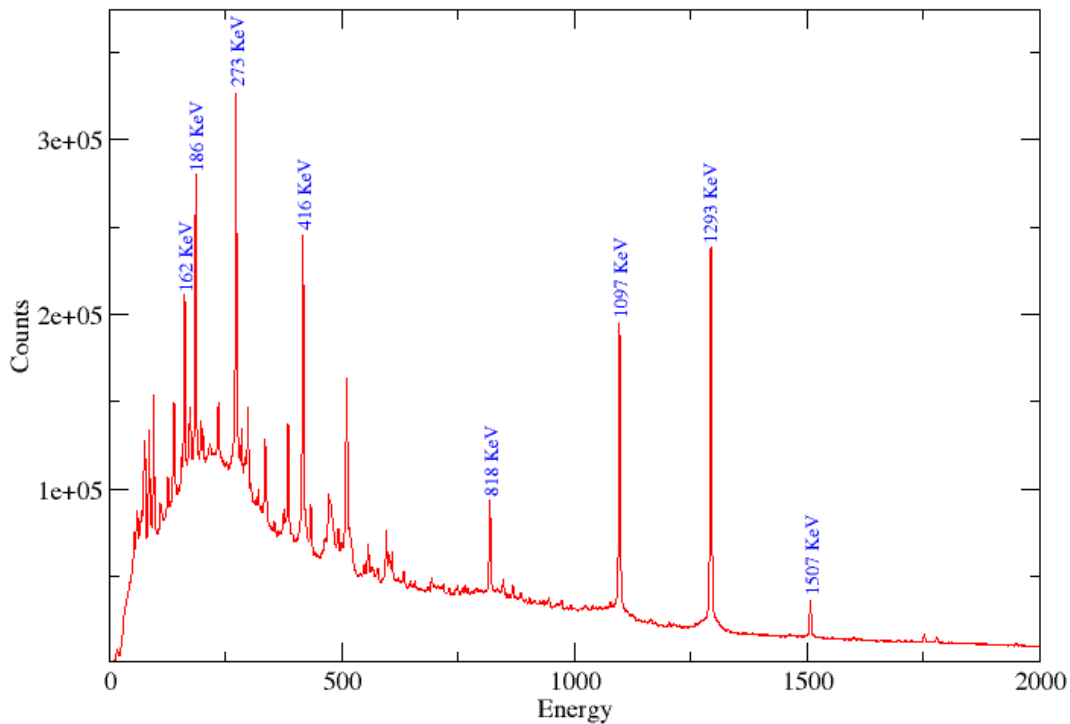
Figure 26: Projection spectra of ^{116}In
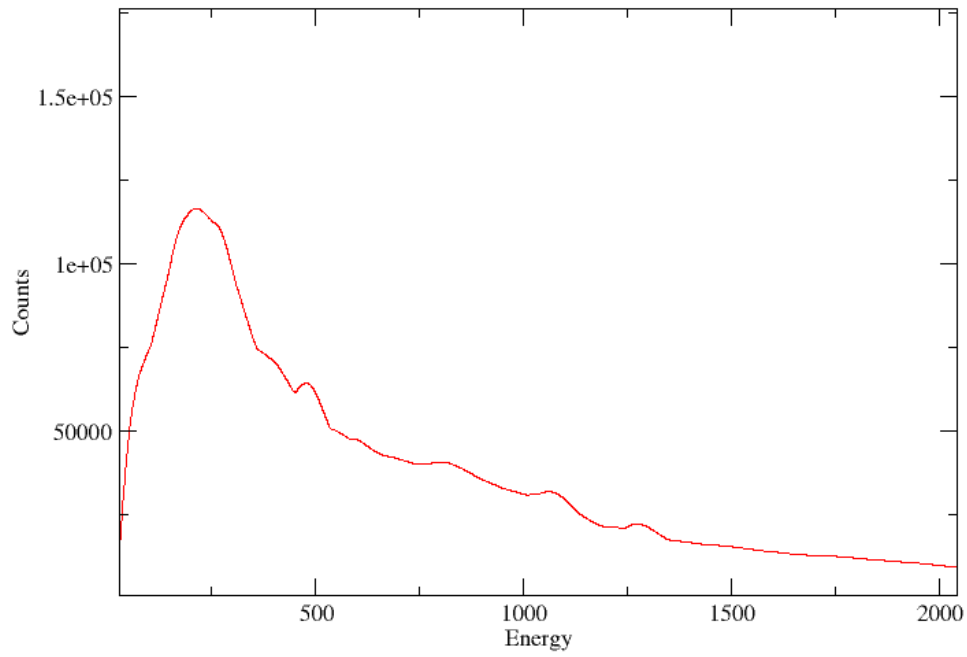
Figure 27: Background spectra of ^{116}In
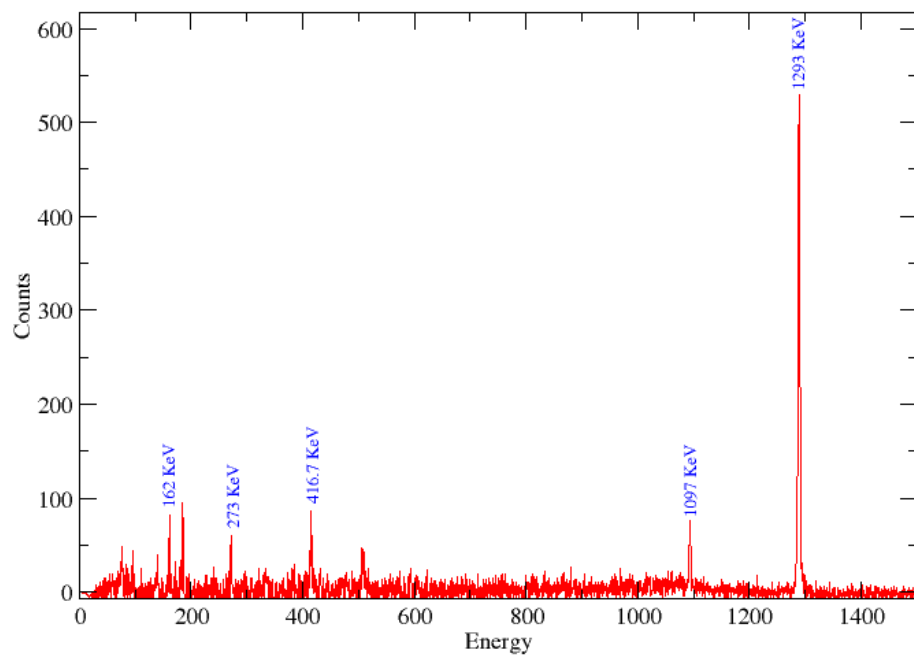
Figure 28: Gated spectra of 1507 KeV gamma of ^{116}In

Conclusion

Gamma-ray spectroscopy is a powerful technique used to study the structure of atomic nuclei by analyzing the energies of gamma rays emitted during nuclear transitions. Through this process, I have learned about different types of radiation detectors, such as scintillation detectors and semiconductor detectors, which are used to detect and convert radiation into electrical signals. The detectors produce analog pulses, which are then amplified, shaped, and digitized to create a spectrum that represents the number of gamma-ray events at each energy level. Calibration spectra are essential for converting the channel numbers of the spectrum into accurate energy values using known sources like ^{152}Eu.

I also explored the creation and use of gamma-gamma coincidence matrices, which help identify cascaded gamma transitions. From these matrices, projection spectra and background spectra can be extracted to better understand the energy distribution and reduce unwanted signals. Gated spectra are particularly useful, as they allow for selective analysis of events that occur in coincidence with a specific gamma-ray peak. Altogether, these tools and techniques help construct nuclear level schemes and provide deeper insight into the discrete energy levels and decay paths of isotopes like ^{116}In. This hands-on learning has strengthened my understanding of nuclear spectroscopy and its role in experimental nuclear physics.

Appendix

A. Python Code Used for Energy Calibration

```python
import numpy as np

# Replace these with your actual data
x = np.array([x1, x2, x3, ..., x10], dtype=float)
y = np.array([y1, y2, y3, ..., y10], dtype=float)

# Fit a quadratic (degree 2) polynomial: y = c*x^2 + b*x + a
coeffs = np.polyfit(x, y, 2)

# coeffs returns [c, b, a] (note the order!)
c, b, a = coeffs

print(f"a = {a}")
print(f"b = {b}")
print(f"c = {c}")
```

Listing 1: Python Script for Energy Calibration using Quadratic Fit

B. Matrix Projection Script for Gamma-Gamma Analysis

```
>INPUT start
>INPUT ipath /home/guest/Desktop/summer_intern_2025/152Eu
>INPUT opath /home/guest/Desktop/summer_intern_2025/matrix
>INPUT cname EuBa_Eff_40MW_VECC_11Feb25
>INPUT run 0
>INPUT bin 0.5
>INPUT end

>TAC start
>TAC file default
>TAC end

>CALIB start
>CALIB file once
>CALIB path /home/guest/Desktop/summer_intern_2025
>CALIB cname Spectrum_Fileparameters.cal
>CALIB end

>MATRIX start
>MATRIX cond all v all
>MATRIX fmatrix
>MATRIX save spn matrix_EuBa_Eff_40MW_VECC_11Feb250000.spn
>MATRIX end
```

Listing 2: Matrix projection script used for gamma-gamma matrix generation

C. Script for Creating Calibrated Spectra

The following script was used to generate calibrated `.spk` spectra files from the raw event data of ^{116}In using the BiNDAS software. It specifies input paths, run numbers, calibration parameters, and output settings.

```
>INPUT start
>INPUT ipath /home/guest/Desktop/summer_intern_2025/In_ng/events
>INPUT opath /home/guest/Desktop/summer_intern_2025/In_ng/calibrated_spks
>INPUT cname In_ng_40MW_VECC_06Feb25
>INPUT run 2, 6, 7
>INPUT calibcomp 0.5
>INPUT end

>CALIB start
>CALIB file once
>CALIB path /home/guest/Desktop/summer_intern_2025/In_ng
          /Spectra_Parameter_files
>CALIB cname eufile_1_spectra_parameters.cal
>CALIB end

>SPEC start
>SPEC crspec clear
>SPEC crspec noadd
>SPEC crspec filelist
>SPEC save spk
>SPEC end
```

Listing 3: Script for Creating multiple calibration spectra

D. Script for Creating Spectra for multiple event files

```
>INPUT start
>INPUT ipath /home/guest/Desktop/summer_intern_2025/In_ng/events
>INPUT opath /home/guest/Desktop/summer_intern_2025/In_ng/calibrated_spks
>INPUT cname In_ng_40MW_VECC_06Feb25
>INPUT run 2, 6, 7
>INPUT end

>SPEC start
>SPEC crspec clear
>SPEC crspec noadd
>SPEC crspec filelist
>SPEC save spk
>SPEC end
```

Listing 4: Script for Creating multiple calibration spectra

References

[1] National Nuclear Data Center. Evaluated nuclear structure data file (ensdf), 2023. URL https://www.nndc.bnl.gov/ensdf/. Accessed: 2025-06-21.

[2] David J. Griffiths and Darrell F. Schroeter. *Introduction to Quantum Mechanics*. Cambridge University Press, 2018.

[3] UW Computational Nuclear Physics Group. Ubuntusetup: How to install windows subsystem for linux (ubuntu) on windows 10. https://github.com/UWCNuclear/UbuntuSetUp, 2025. GitHub repository, accessed on June 28, 2025.

[4] Glenn F. Knoll. *Radiation Detection and Measurement*. John Wiley & Sons, 2010.

[5] Kenneth S Krane. *Introductory nuclear physics*. John Wiley & Sons, 1991.

[6] LibreTexts. Particle in a 1-dimensional box, 2025. URL https://chem.libretexts.org/Bookshelves/Physical_and_Theoretical_Chemistry_Textbook_Maps/Supplemental_Modules_(Physical_and_Theoretical_Chemistry)/Quantum_Mechanics/05.5%3A_Particle_in_Boxes/Particle_in_a_1-Dimensional_box. Accessed: 2023-11-15.

[7] Paul Lutus. Polysolve: Polynomial root calculator, 2025. URL https://arachnoid.com/polysolve/. Accessed: 2025-06-21.

[8] Satya Samiran Nayak. Bindas installation and usage manual, 2025. Available upon request.